International Journal of Thermofluids 30 (2025) 101450

Contents lists available at ScienceDirect

International Journal of Thermofluids

journal homepage: www.sciencedirect.com/journal/international-journal-of-thermofluids

A review of industrial pumps for viscous and non-Newtonian slurry transport

Oscar Ifidon [a], Daya Shankar Pandey [b], Khurshid Ahmad [c], Artur J. Jaworski [d], Faisal Asfand [a,*]

[a] School of Computing and Engineering, University of Huddersfield, Huddersfield, UK
[b] School of Mechanical Engineering, University of Leeds, Leeds, UK
[c] USPCASE, University of Engineering and Technology Peshawar, Pakistan
[d] School of Engineering and Design, London South Bank University, London, UK

ARTICLE INFO

Keywords:
Non-Newtonian fluids
Rotodynamic
Tesla disc pump
Viscous flow
Multiphase flow

ABSTRACT

This paper presents a concise review of industrial pumps for viscous and non-Newtonian slurry transport. It combines both the computational fluid dynamics (CFD) and experimental analysis to investigate the performance and limitations of various rotodynamic and positive displacement (PD) pumps for various slurry transport applications. The factors influencing head, efficiency and reliability in rotodynamic and PD pumps were evaluated for viscous and non-Newtonian fluids applications. Available literature showed that centrifugal pumps experience head losses of $\geq$ 8 m and efficiency reduction of 20 % when viscosity approaches 800–1000 cP, whereas the blade and volute optimisation could improve the overall efficiency. The performance of the multiphase pump showed a sharp decline when handling non-Newtonian fluids, primarily due to the formation of complex vortex structures and tip-leakages. This study also highlighted key geometric parameters for optimisation to improve overall performance and enable the integration of multiphase pumps as a prime mover in a jet pump system, for a robust handling of highly viscous and solid-laden fluids. While the special-effect jet pumps had lower peak efficiencies compared to other rotodynamic pumps, robustness and passability for abrasive and multiphase flows were demonstrated, achieving up to 40 % efficiency in sand slurry applications. PD pumps, such as the reciprocating plunger and diaphragm designs, exhibited the highest viscosity tolerance, however, their performance was limited by valve response and mechanical complexity. This review particularly focused on the capabilities of Tesla disc pump for handling highly viscous and abrasive fluids. Literature on Tesla disc pumps emphasised that geometric optimisation of the disc impeller, combined with the use of a dedicated volute, could significantly enhance its efficiency and position it as a complementary solution to both centrifugal and PD pumps. The analysis of life cycle cost (LCC) showed that the Tesla disc pump maintained moderate costs for harsh applications, indicating a sustainable operational life cycle.

1. Introduction

Pumps are among the most common machines in industries today, and their application can be found in every industrial processing environment, essential for transporting various fluids. Moreover, a vast number of special pumps are designed to handle a variety of simple and complex fluids. Since most industries require pumps as a source of fluid transfer from one place to another, there is a progressively high demand for pumps with high efficiency and reliability, cost-effectiveness and low maintenance for diverse applications [1]. Pumps are classified into two main categories - rotodynamic and positive displacement (PD) pumps. Pumps are categorised based on their mode of operation, as shown in Fig. 1. Rotodynamic pumps are velocity-based pumps that add kinetic energy to increase the flow velocity of the resulting fluid, while PD pumps are flow-based pumps that trap and release a specific volume of fluid [2]. In rotodynamic pumps, kinetic energy is generated through the interaction of moving or stationary components, whereas in PD pumps, it arises from reciprocating or rotational mechanisms. Typical rotodynamic pumps that generate kinetic energy by moving parts are called centrifugal pumps. The principal difference between PD pumps and rotodynamic pumps are based on the concept that PD pumps generate steady flow regardless of the pressure differences, while rotodynamic pumps create pressure by adding velocity to the fluid flow. Hence, when there is a change in pressure, there is a corresponding change in flow

* Corresponding author.
E-mail address: f.asfand@hud.ac.uk (F. Asfand).

https://doi.org/10.1016/j.ijft.2025.101450

Available online 10 October 2025

[3].

The general concept of PD pumps in idealised cases can be expressed as:

$$\text{Volumetric flow rate, } Q = n.C \quad \text{(I)}$$

$$\text{Power, } N = \left(\frac{(2.p + V)nC}{1000}\right)kW \quad \text{(II)}$$

$$\text{Efficiency, } \eta = \frac{Q_{actual}}{Q_{theoretical}} \times 100\% \quad \text{(III)}$$

The general concept of Rotodynamic pumps in idealised cases can typically be expressed as:

$$\text{Volumetric flow rate, } Q = \frac{\pi D^2 nH}{4g} \quad \text{(IV)}$$

$$\text{Head, } H = \frac{U_2 V_{w2} - U_1 V_{w1}}{g} \quad \text{(V)}$$

$$\text{Efficiency, } \eta = \frac{Output}{Input} = \frac{pgQH}{P} \quad \text{(VI)}$$

Where *H*representshead, *Q* is the volumetric flow rate, *N* is the power, *n* is the pump speed, *C* is the displacement volume for revolution or stroke, *p* is the pressure, *V* is the viscosity factor, *D* is the impeller diameter, *g* is the acceleration due to gravity, *U* is the tangential velocity (rotor speed) and V_w is the whirl velocity.

In comparison, PD pumps are essential for applications that require steady flow at varying pressure, while rotodynamic pumps are essential for applications that require steady pressure at varying flow rates. However, fluid complexity impacts the pressure of rotodynamic pumps, which could cause some loss in efficiency. PD pumps are extensively used for complex fluids, as in oil rigs [4], mining [5], fertiliser industries, food, etc. [6]. The major drawbacks of commercial PD pumps are their complexities, high energy cost [5] and difficulty in maintenance. These pumps have a characteristic low flow rate compared to the rotodynamic pumps. However, PD pumps deliver a steady flow at a fixed RPM and have a relatively outstanding working efficiency at different speeds [7, 8].

Centrifugal pumps are typically radial flow pumps, although the term centrifugal pump is used to categorise other impeller-based rotodynamic pumps such as axial flow pumps, mixed flow pumps, and peripheral pumps [8]. Typical centrifugal pumps, as shown in Fig. 2, are efficient for various low-viscosity applications such as water projects, sewage, chemical plants and oil refineries [9]. However, centrifugal pumps encounter efficiency issues when handling highly viscous and non-Newtonian fluids due to their close tolerance and inability to produce a shear-thinning effect when lifting thixotropic fluids, hence, the pump gets power-thirsty, promoting vibration and clogging [10].

In axial flow pumps, as shown in Fig. 3a, fluid flows axially from the inlet and is discharged from the pump axially through the outlet by the action of a rotating fan-like impeller, which is otherwise referred to as a propeller [12]. Due to the pump design, fluid flows in a swirl motion along a path parallel to the axis of the pump, where swirl motions are minimised by the guide vane. Axial flow pump has a characteristic high flow rate and low head due to its large flow area and small impeller diameter relative to other rotodynamic pumps. It has a vast application in aerospace industries as it appears to be primarily applied in the production of compressors in turbo-jet engines [13], since its distinct advantage is its high flow delivery. A mixed flow pump combines the characteristics of a traditional centrifugal pump (radial flow design) and an axial flow pump, and are smaller than axial flow pumps but run at higher speeds [14]. The mixed flow pump design has a single impeller, which is a hybrid of axial blades facing the inlet and radial guide vanes facing the outlet [15] as shown in Fig. 3b. Mixed flow pumps are often suitable for high flow rates and medium heads of about 7 m to 16 m, depending on the specification [16]. They are widely applied in sewage, water circulation farming, industrial water [14], thermal power plants for cooling water [17], drainage pumping, and canal pumping. The regenerative pump, known as the peripheral pump, as shown in Fig. 3c, is similar to a standard centrifugal pump. It operates by exerting kinetic

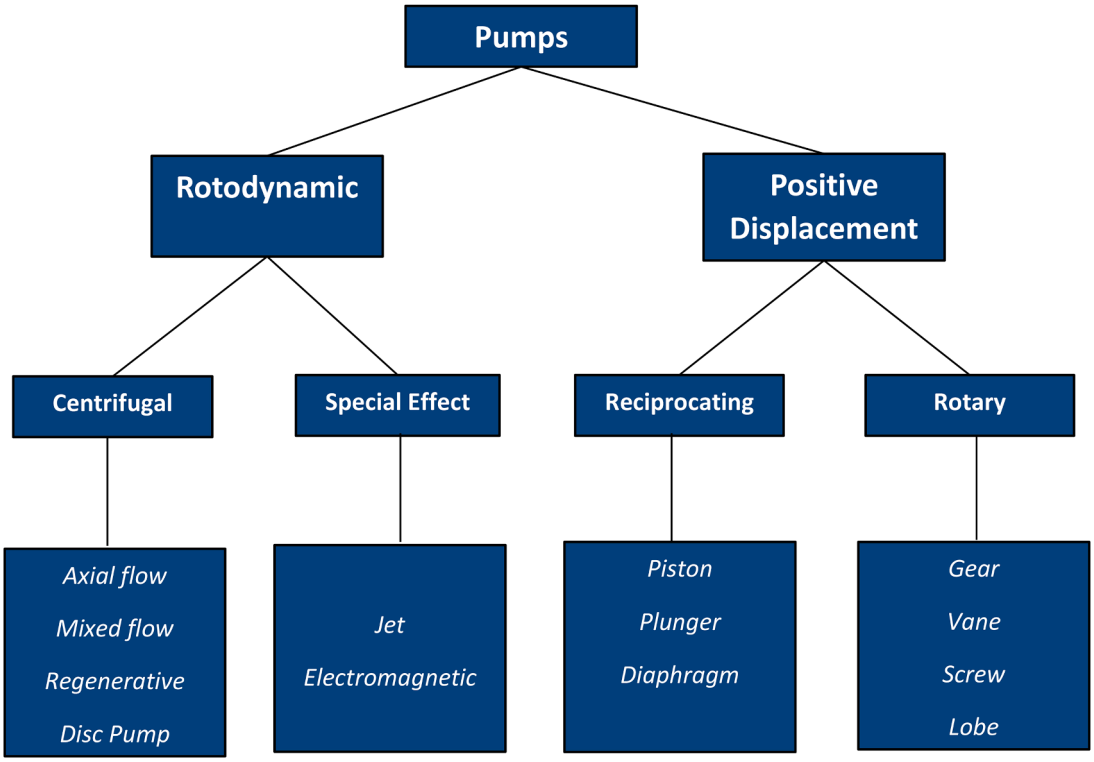

Fig. 1. Classification of pumps based on their working principle.

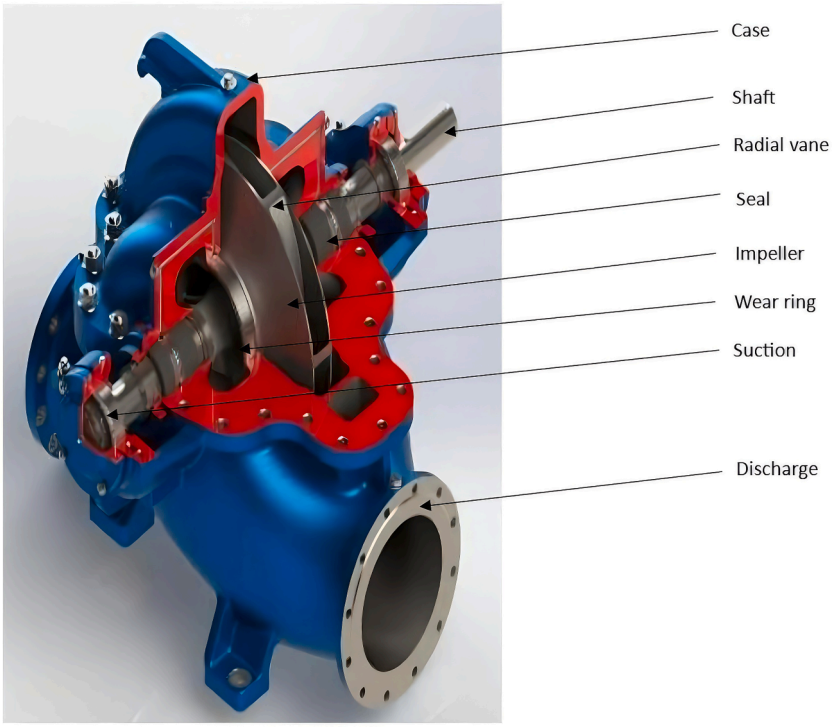

Fig. 2. A typical close impeller centrifugal pump [11].

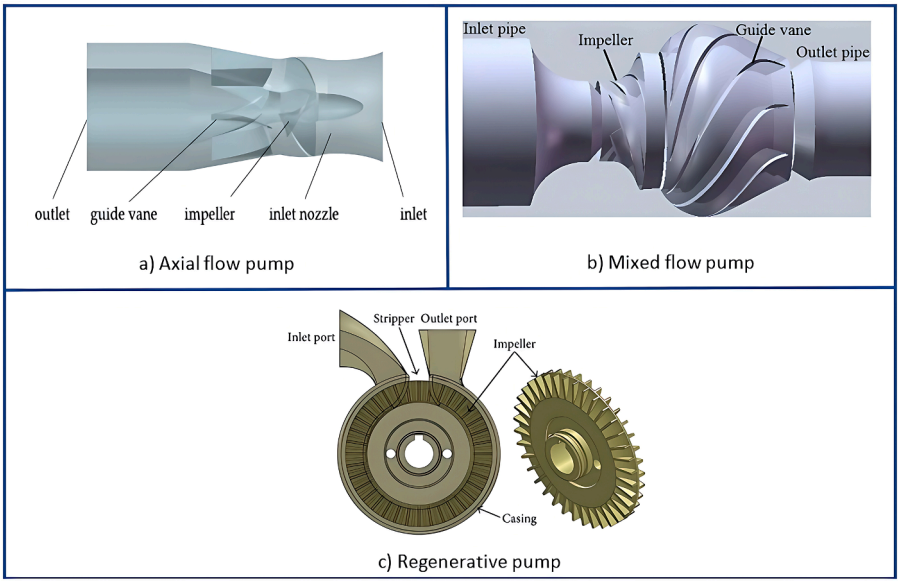

Fig. 3. Diagram of axial flow, mixed flow and regenerative pump [18–20].

energy on the fluid using a rotating impeller.

The impeller of the regenerative pump consists of radial teeth or vanes machined on the circumference of the impeller rim [21]. The regenerative pump consists of an inlet and an outlet separated by a barrier called the stripper [21]. The pump's casing has a ring-like structure [22], which creates an annular channel for fluid to enter and leave the pump. The major characteristic of the regenerative pump is its ability to lift fluid at a high head, low flow rate, and low specific speed due to its repeated fluid circulation before discharge [21,22]. The regenerative pump delivers the highest head value amongst other dynamic pumps when set to work at the same operating conditions. However, it declines in efficiency, which ranges from 35 % to 50 %, due to hydraulic losses such as tangential head loss at the side channel, incidence loss due to the difference in blade and flow angles, impeller loss due to friction, contraction and abrupt expansion [21]. However, the regenerative pump's characteristics and relatively low manufacturing cost have led to vast industrial applications such as automobiles, aircraft fuelling pumps, industrial agriculture, shipping and mining, and food processing systems [21,22]. The special effect pump is another branch of a rotodynamic pump that adds kinetic energy to the fluid through special effects requiring no moving parts. Based on the special effect added, special effect pumps can be categorised as jet and electromagnetic pumps. The jet pumps are most efficient in lifting incompressible fluid from a bore of varying depths. However,

applications where a compressible constituent of unequal density is present are accounted for by optimising the flow rate and friction loss coefficients to suit the requirement [23]. Fig. 4a shows a jet pump that works by pumping fluid simultaneously at high pressure and velocity with the aid of a jet mechanism immersed in the bore; as a jet of fluid flows down the bore, a corresponding flow of fluid is forced upwards [23]. The major drawback of this pump is its characteristic low head, which leads to low efficiency for a high-head application [24]. However, since it has no moving component, the problem of wear due to dynamic resistance is not present, and the cost of production is relatively low. They are widely applied in chemical manufacture, oil, gas production, and nuclear engineering [24]. As investigated by Michael Faraday in the 1800s [25], the electromagnetic pump, as shown in Fig. 4b, operates by the action of electromagnetic fields, which obeys the same principle that governs an induction motor. The magnetohydrodynamics of the pump obeys the right-hand rule; thus, induction due to chirality or opposite polarity relative to the pumping fluid results in fluid movement from the electromagnetic field to the outlet [25]. The electromagnetic pump is sectioned into two types: conduction and induction pumps [25]. In conduction pumps, there is a direct interaction between the current and the fluid, while induction pumps indirectly induce motion to the fluid with no direct contact as the fluid is lifted by pure induction from the electromagnetic field [26]. The electromagnetic pump is simple in structure and does not require an impeller to generate energy [27]. They are essential for lifting hazardous fluids, which could damage a typical pump and result in a risk of uncontrolled fluid escape. Some examples of these fluids are liquid metals, chemicals and hot radioactive liquids [25,27]. The major drawback, which has led to the non-use of this pump, is an extreme case of low efficiency due to a significantly low flux density in the electromagnetic field. Thus, excessive electrical power is required for fluid discharge [27].

The PD pump is a category of pump different from rotodynamic pumps. They work by trapping a certain quantity of fluid from the inlet and releasing them through an outlet by utilising check valves arranged in series. They consist of at least one valve each at both the inlet and outlet [30]. Generally, PD pumps lift fluid from the region of low pressure (suction) to the region of high pressure (discharge) [31]. Unlike rotodynamic pumps, PD pumps have constant flow at a given speed. Based on the fluid's lifting mechanism, the PD pump can be categorised into reciprocating and rotary types [30]. The reciprocating pump works like an internal combustion engine. It consists of a piston positioned in a chamber and at least one valve at both the inlet and outlet. The reciprocating pump is defined based on its actuating mechanism. They may be a piston, plunger, or diaphragm pump, as shown in Fig. 5; however, they all work by a similar principle.

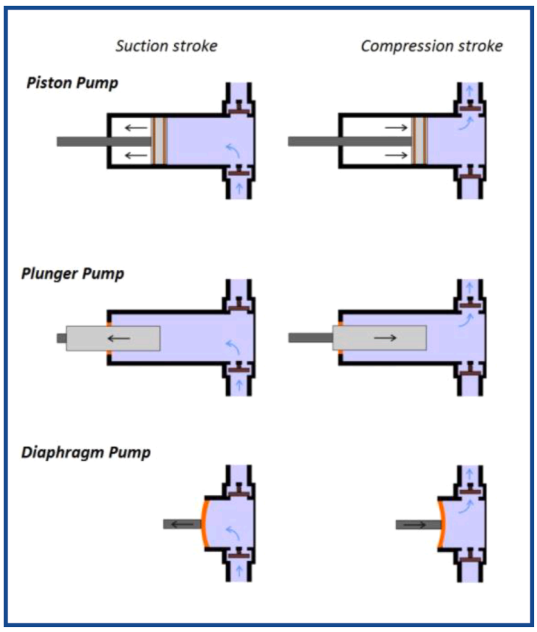

Fig. 5. Piston, plunger and diaphragm positive displacement pump reprinted with permission from Ref. [32].

On the other hand, the rotary pump operates by a rotational motion. As the actuating components rotate, a vacuum that siphons and traps fluid is created at the suction region and released at the discharge region at a higher pressure [33,34]. The rotary pumps have different design mechanisms, which are sectioned into single-rotor and multiple-rotor pumps. The single-rotor pump has a single suction vacuum per revolution, while the multiple rotors typically have several suction vacuums per revolution [34]. Some of the rotary pump types, as shown in Fig. 6, include the external gear pump, internal gear pump, lobe pump, and vane pumps.

As shown in Fig. 7, the Tesla disc pump is a type of rotodynamic pumps. It operates by the action of boundary layers and viscous drag generated by the rotation of disc impellers, intended to lift the pumping fluid [35,36]. It is essential for hard-to-pump applications such as high-suspension solids, abrasive and viscous fluids, shear-sensitive and air-entrained fluids. They usually work at high inlet pressure to prevent cavitation conditions. The rotation of the disc impeller generates a surrounding buffer due to viscous drag and boundary layers. The buffer tends to minimise the pump-to-fluid contact. Thus, reducing the

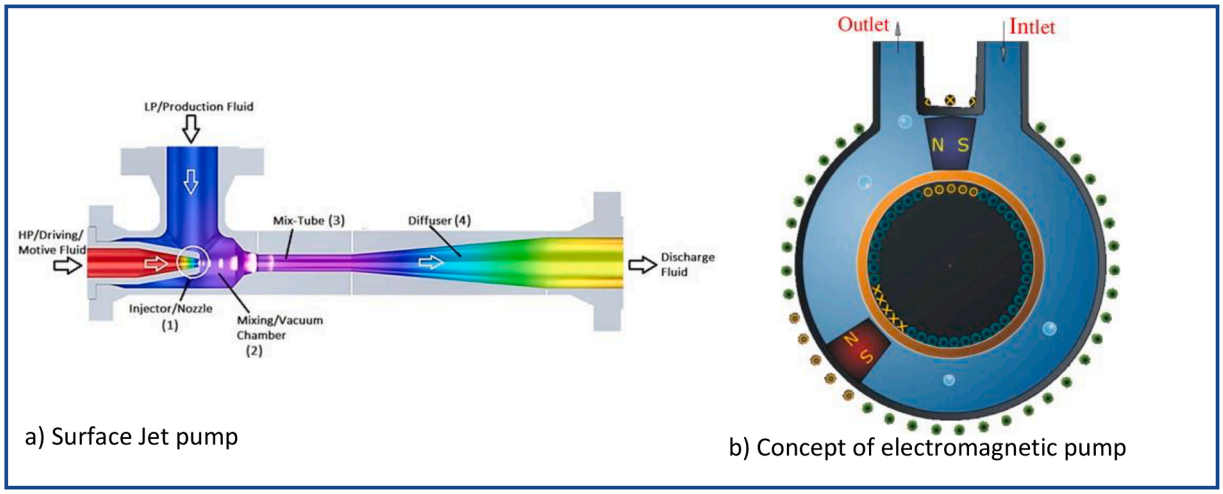

Fig. 4. Surface jet pump and the electromagnetic pump reprinted with permission from Ref. [28,29].

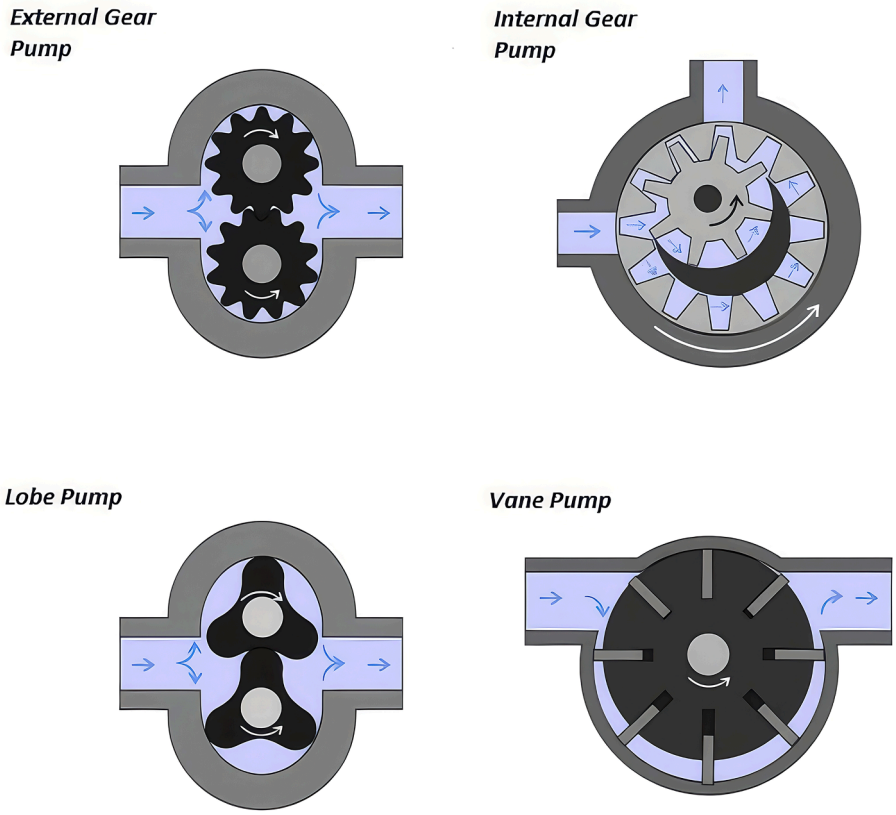

Fig. 6. Common rotary positive displacement pumps reprinted with permission from Ref. [32].

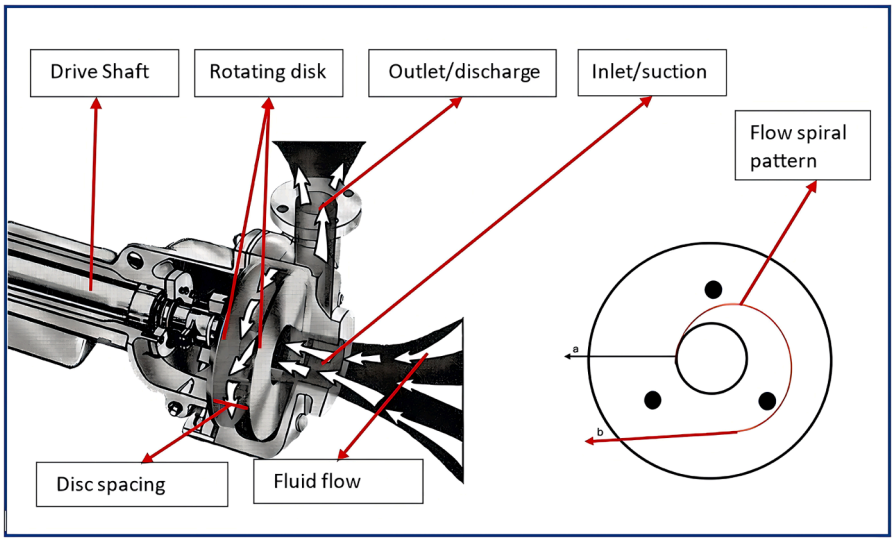

Fig. 7. Tesla disc pump [37].

tendency of impeller damage and vibrations, they further maintain the fluid integrity [36]. Moreover, the disc impellers have simple designs [37]. Due to the simplicity of the impeller design, the Tesla disc pump has a characteristic low efficiency compared to other pumps of similar applications, which is a major drawback that contributes to its limited use in industrial applications [38].

For vast industrial applications, handling delicate and hard-to-pump fluids such as highly abrasive fluids with solid constituents, non-Newtonian fluids with high viscosity, and entrained gases are increasing problem for pump applications. Lifting these fluids may impart significant damage to pump impellers. Furthermore, impeller clogging and degradation of the exotic fluid may occur. Although the PD pumps efficiently handle a vast range of delicate fluids, the structural complexity and size pose a maintenance and compatibility problem. The simple disc pack and buffer effect of the Tesla disc pump is unique among the PD and centrifugal pumps. The Tesla disc pump trades off low maintenance cost and better reliability for problem-fluid at the expense of low overall efficiency. Nevertheless, this study concluded that optimising the impeller structural design can significantly augment the overall efficiency of the Tesla pumps.

The introduction section provides an overview of pump technologies with emphasis on their working principles, operational characteristics and suitability for various fluids in industrial applications. Therefore, the selection of pump type should be guided by fluid properties, required flow rate and head, as well as specific application demands, including operating and maintenance costs. While rotodynamic pumps are preferred for high-flow, low-viscosity applications, PD pumps excel in handling complex and high-viscosity fluids. The Tesla disc pump, a type of rotodynamic pump, shows potential for efficiently handling complex and high-viscosity fluids at relatively low operating and maintenance costs. Ongoing improvements in the structural optimisation of Tesla disc pumps are addressing longstanding challenges in efficiency and reliability to further enhance their suitability for demanding industrial processes.

The subsequent sections are organised to employ a literature review of CFD and experimental analyses assessing the geometric optimisation of wetted components, such as the volute and impeller, and the performance of centrifugal and PD pumps, particularly in viscous and abrasive fluid applications. The study highlights the Tesla disc pump as a promising solution for handling viscous and abrasive fluids and demonstrates that optimising internal geometries can significantly enhance global efficiency. Overall, the findings underscore the critical role of geometric optimisation in improving pump performance to inform future design strategies, with particular emphasis on the potential of Tesla Bladed Disc pumps.

The last section represents a LCC analysis comparing rotodynamic and PD pumps under low-viscosity conditions, highlighting maintenance and operational costs. It also evaluates the performance and maintenance of Tesla disc pumps under viscous and abrasive applications to demonstrate their cost-effectiveness and durability in rising industrial demands.

2. Review of industrial pumps for viscous, non-Newtonian, and abrasive slurry transport

2.1. Centrifugal pumps

When a typical centrifugal pump operates with highly viscous and abrasive fluid, it becomes susceptible to cavitation, accompanied by noise and vibration, clogging and abrasive impingement on the impeller. Such a condition can result in rapid corrosion, pressure losses or complete shutdown of the pump. It was stated that centrifugal pumps typically handle a maximum viscosity of 800 cP [39]. Moreover, since centrifugal pumps are incapable of shear thinning, they underperform with non-Newtonian fluids owing to their thixoplastic properties.

Researchers have found that pump geometry can significantly influence its performance, and modifying the geometry of the wetted area directly impacts efficiency across a variety of applications. Uchida et al. [40] experimented on the geometry of a centrifugal pump using six different volute tongue designs, which had different shapes and areas. The study was intended to quantify how the designs affect the characteristics and radial forces of a typical centrifugal pump. It was found that the smaller volute tongue area delivered higher hydraulic efficiency in the pump. Furthermore, the different shapes of the volute tongue were found to have affected the pump efficiency in the different capacity regions. In terms of radial force, it was reprorted that the magnitude of radial force varied relative to the volute tongue shape due to the variation in flow discontinuity at the cut-off. In contrast, the volute tongue area did not affect radial force in the pump. Zhou et al. [41] concluded that optimisation of impeller vanes by skewness, length and angle variation can improve pump efficiency because the energy loss due to flow recirculation can be minimised. Furthermore, Uchida et al. [40] reprorted that the impeller was not perfectly matched with the volute, resulting in a non-uniform flow across the pump. Consequently, the volute tongue was used to measure the radial force present in the pump. At higher flow rates, there was a significant level of instability due to a non-cyclic wave that originated from the imperfect volute to impeller coupling. The pump capacity was reduced to acquire more stable results of radial force, hence creating some limitations in analysing radial efficiency at high-capacity zones. However, results of the tongue area and shapes showed some elaborate pump characteristics at a low-capacity range, which demonstrated that the different tongue geometries significantly affected the pump head and efficiency. Moreover, the cavitation phenomenon can occur at high-capacity regions, as illustrated in Fig. 8, which depicts the phenomenon of cavitation at the volute tongue region. The inception of the cavitation bubbles occurred at the leading edge, which advanced and detached as the spindle torque increased, resulting in cavitation shedding, which progressed to cavitation wake. When centrifugal pumps add kinetic energy to flowing fluid, limitations can occur if the fluid to impeller slip is not optimised.

From Zhou et al. [41] CFD investigations, it appeared that the flow recirculation in the centrifugal pump strengthened the rate of turbulence at the impeller region, which led to a predominant flow slippage at various impeller regions. The CFD analysis presented straight and curved impeller vanes, which showed some backflow in the velocity vector. Although the analysis of the impeller vanes was precise, the impeller diameter and the impeller-to-volute relationship were not stated. A relatively small impeller and an imperfect impeller-to-volute matching may significantly affect the results in this analysis. Buratto et al. [43] performed a CFD analysis of an industrial centrifugal pump designed for tomato application. Three categories of fluid were tested with the pump. The authors included a fluid with low viscosity (water), a non-Newtonian fluid (Tomatoes), and a highly viscous fluid (virtual fluid). The analysis demonstrated a similar flow characteristic between a non-Newtonian fluid and a Newtonian fluid with high viscosity, which shows how they differ from fluids with low viscosity in the centrifugal pump application. Compared to the fluid with low viscosity, the thermodynamic properties and increase in viscosity of both viscous and non-Newtonian fluids resulted in high disc friction and shaft power loss by 17 %. Consequently, there was a decline in the best efficiency point (BEP) and head for viscous and non-Newtonian fluids. Their head and global efficiencies ranged from 28 m-34 m and 58 %−65 %, respectively. In comparison, the fluid with low viscosity reached a head of 36 m with a global efficiency of 86 %. It is evident that augmented fluid viscosity and viscoelasticity significantly affected the performance of a typical centrifugal pump. However, there was a contradiction by Onica et al. [44] who stated that the viscoelasticity of a non-Newtonian fluid can significantly improve or strengthen flow behaviour due to molecular stretching and coiling. The study was conducted at a microscale of viscoelastic fluid flow through micro channels, while Buratto et al. [43] referred to the fluid lifted by a commercial pump. In comparison of both ideas, it can be deduced that viscoelasticity in non-Newtonian fluid has a characteristic high energy transfer due to molecular stretching. However, this is a problem in typical centrifugal pumps as the close tolerance between the impellers and volute walls will result in viscoelastic resistance, which could limit the impeller efficiency by causing mechanical losses. Zaman et al. [45] investigation showed that the major drawback of a typical centrifugal pump is the predominant hydraulic loss, which reduces efficiency during viscous and non-Newtonian applications. The hydraulic losses caused by high viscosity in centrifugal pumps are due to friction concentration in the flowing fluid [46]. When efficiency begins to drop, cavitation and clogging may be promoted, leading to pump failure [42]. Torabi et al. [47] added that a high-performance centrifugal pump with enhanced impellers could handle viscosities within 520 - 760 cSt but is unsuitable for fluid viscosities exceeding 1000 cSt. The CFD study, as shown in Fig. 9, depicts the velocity vector at the suction region of the pump for both water and oil applications, where the oil viscosity was 90 cSt. Some vortices were observed around the wear ring in both applications, and the vertex region appeared larger in the oil application. This indicates some disc friction losses at the sidewall gap, and hydraulic loss originating from friction and turbulence concentration, which worsened as fluid viscosity increased.

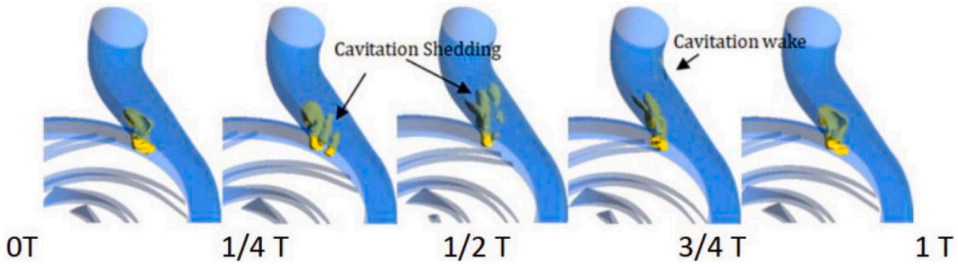

Fig. 8. Cavitation characteristics at the volute tongue as impeller torque increases [42].

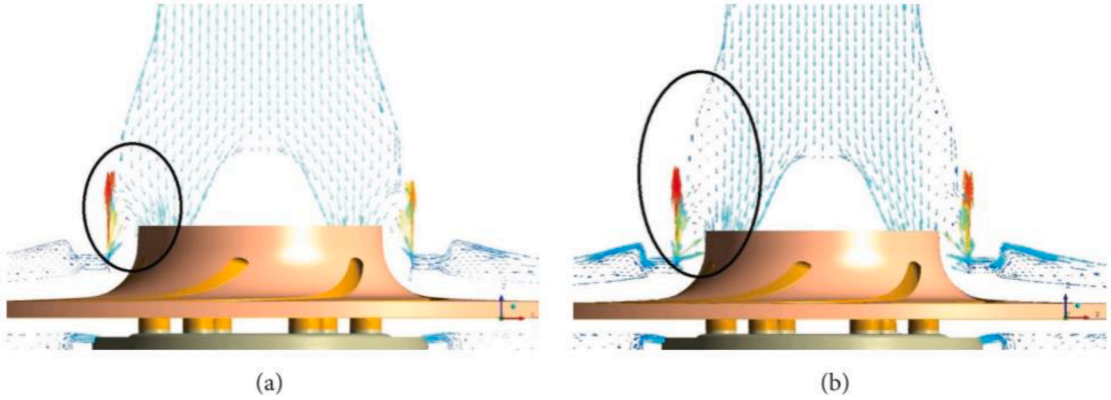

Fig. 9. Velocity vector of leakage flow at the impeller suction - a; water, b; viscous oil [47].

The experimental and CFD investigation, described in Fig. 10, quantifies the pump efficiency (η) and power (π) requirement between water and oil applications across a range of mass flow rate (φ). It demonstrates a higher power requirement in the oil application, and a decline in the BEP by 20 % when lifting the viscous oil, illustrating that the increase in fluid viscosity led to hydraulic losses in the impeller rotating zone. Owing to the design of a typical centrifugal pump, a remarkable performance for fluid with low viscosity is evident as global efficiency and head climb up to 86 % and 36 m, respectively. Centrifugal pumps have low tolerance for handling highly viscous and non-Newtonian fluid due to hydraulic losses, flow slippage, cavitation, clogging and recirculation [43]. Torabi et al. [47] also demonstrated a decline in global efficiency by 20 % head losses from 34 m to 28 m for highly viscous oil application.

The study of the geometry in the wetted area of the centrifugal pump provides valuable insight into the design optimisation required to improve performance in viscous fluid applications for slurry transport. The key design parameters for improvement include adjusting the volute tongue area to stabilise radial forces and enhance hydraulic efficiency, lengthening of impeller vanes and optimising dimensional vane angles to minimise recirculation, strategically increasing the internal clearance to minimise clogging and viscoelastic resistance.

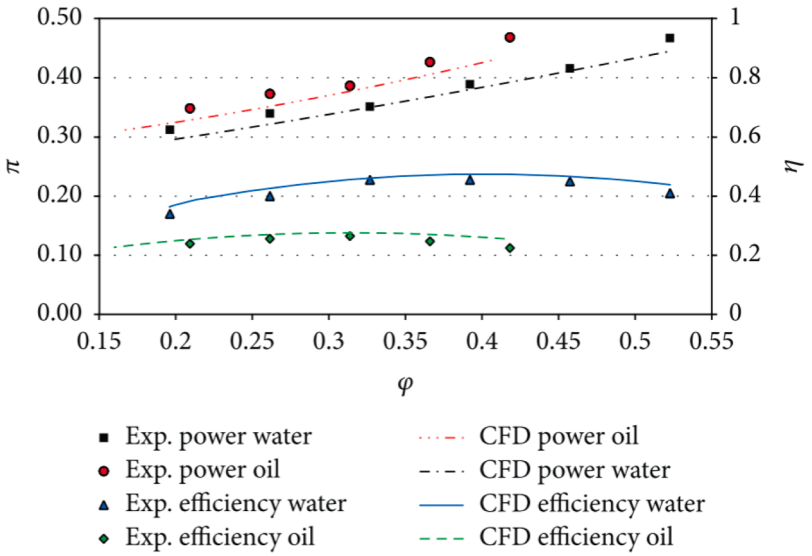

Fig. 10. Effect of fluid viscosity on efficiency and shaft power of an optimised centrifugal pump, reprinted with permission from Ref. [47].

2.2. Multiphase pump

A typical multiphase pump is shown in Fig. 11. Liu et al. [48] carried out a CFD-based study on the impact of viscosity on the flow field and energy performance of a multiphase pump.

The study was based on a three-stage helico-axial multiphase pump where water and three grades of glycerol with viscosities of 0.1, 0.2 and 0.3 kg.m/s were used as the working fluid for each test. The study was focused on the influence of viscosity, flow rate and blade height on the distribution of turbulence kinetic energy. The analysis showed that an increment in viscosity resulted in a corresponding decline in flow rate, leading to a rise in the turbulent kinetic energy. The result demonstrated that the optimum flow rate of water had the highest head and efficiency of 1.43 m and 50 %, respectively, whereas glycerol, with a viscosity of 0.3 kg.m/s had the lowest head and efficiency of 1.1 m and 20.5 %, respectively, as demonstrated in Fig. 12. Although the authors clearly described the limitations of the multiphase pump when handling viscous fluid, nevertheless, only limited details on the structural factors that affect the multiphase pump during viscous application were discussed.

An internal flow analysis on the length of the impeller blades shown in Fig. 13a and b illustrates a visible quantity of tip leakages on each blade, indicating an increased vortex induced at the blades' leading and trailing edges [50]. It is expected that the increase in fluid viscosity exacerbates the induced turbulence and entropy, leading to a decline in head and efficiency.

CFD analysis showed good hydraulic performance for gas lifting, revealing a uniform flow pattern in the impellers of the multiphase pump [48]. Hence, multiphase pumps are more efficient with gaseous and low-viscosity liquids compared to viscous liquid-solid flow.

To have a holistic view of the pump performance with various fluid categories, further CFD and experimental studies were critically reviewed to compare the hydraulic performance, vortex structure evolution and induced pressure fluctuation when handling non-Newtonian (carboxymethyl cellulose and bentonite mixture) and viscous Newtonian fluids (seawater) [51]. Fig. 14 describes the graphical analysis of apparent viscosity and shear strain rate – y-axis, across the axial flow path (z/m) – x-axis, of the multiphase pump. At the ingress of fluid into the impeller, the buildup of kinetic energy results in an increase in fluid velocity, leading to a corresponding spike in the shear strain rate around $57.5\mu_e/mPa.s$ at $z/m = 0.05$ and a two-stage sharp reduction interrupted by a transitional flow from the leading edge to the trailing edge due to the shear thinning of the fluid. Fig. 14 further shows that on approaching the diffuser from $z/m = 0.06$, the shear strain rate exhibits low amplitude oscillations but eventually surpasses the value at the impeller leading edge around $z/m = 0.008$ as it advances to the exit at $z/m = 0.13$. This increase is attributed to a drop in kinetic energy and a corresponding rise in pressure. Moreover, it is notable that the transitional behaviour in the shear strain rate exhibited a clear inverse relationship with the apparent viscosity. Specifically, the shear strain rates were in the range of approximately 1700 – 3300 1/s in the diffuser region, which corresponded to significantly lower apparent viscosity values compared to those at the impeller region. Whereas the shear strain rates around 700 1/s to 4500 1/s were observed at the impeller region, where the apparent viscosity was relatively higher compared to the diffuser region. The increase in viscosity indicates the presence of flow instabilities and vortices within the impeller, as demonstrated earlier.

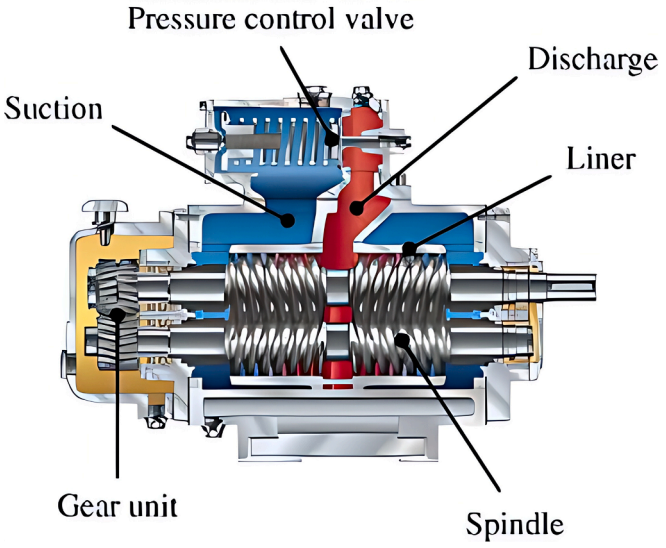

Fig. 11. Multiphase pump reprinted with permission from Ref. [49].

Fig. 15 utilises CFD to further analyse the internal flow instabilities in the impeller when applied to the viscous Newtonian and non-Newtonian fluid. At the blade trailing edge D1, the vortex structure for the non-Newtonian fluid emerged as two separation vortices (vortex A and vortex B), while the viscous Newtonian fluid exhibited a single separation vortex (vortex C), which was subsequently dissipated into smaller cascades. The pressure fluctuation was significantly influenced by the fluid thixotropy, which worsened during the non-Newtonian fluid application.

While multiphase pumps offer strong performance and good passability for gas-liquid mixtures and low-viscosity fluids, they face efficiency and operational challenges with highly viscous or solid-laden slurries. Parametric optimisation in blade geometry, tip clearance and material choices can help broaden the pump application and improve efficiency in more demanding conditions. Although the multiphase pump struggles with efficiency when handling solid-laden slurry, it can be applied as a prime mover that drives a jet pump system for lifting dense slurry more effectively, where the multiphase pump generates a robust flow and pressure, and the jet pump, having no moving parts, can transport dense slurry more effectively.

2.3. Special effect jet pump

Fujita et al. [52] explored the characteristics and potential of the jet pump on viscous non-Newtonian fluids. The investigation was supported by an experimental study of a steam jet pump for oil recovery and reformation. In the experiment, water steam supplied the motive fluid to the jet mechanism. The pump was used to lift various fluids, including the emulsion of water in bunker-C oil, a multiphase mixture of bunker-C oil with sand slurry and air. The experimental results showed that the pump efficiently handled highly viscous emulsified oil, due to the influence of elevated temperature from the steam, which reduced the oil viscosity. Furthermore, emulsification of immiscible mixtures was observed during the pumping process without a chemical reagent or surfactant acting on them. The pump lifted both liquid and sand slurry with high suction power. For a wider range of performance, it was suggested that higher pump efficiency could be attained by optimising the space between the mixing tube and nozzle, and adapting the nozzle dimensions [53]. Table 1 outlines the parametric analysis of key geometric parameters and quantifies their performance on the jet pump configuration, operating with viscous emulsified fluid. The parameters include the mixing tube diameter (d_m), area ratio (R), referring to the ratio of the cross-sectional area of the mixing tube to the nozzle, and spacing between nozzle and mixing tube (S). For each configuration series from 1 to 5, the corresponding discharge ratio (M), which refers to the ratio of the total discharge flow rate, the pump head ratio (N) and the BEP were quantified. The trend shows that the increase in the mixing tube diameter (d_m) resulted in a corresponding rise in the discharge ratio (M), pump head ratio (N) and the BEP%. However, the maximum efficiency reached was 25.1 % which is notably low compared to centrifugal pumps. A comparable experimental study was carried out by Jia et al. [54] on the significant geometric parameters that could augment the efficiency of the jet pump for sand flushing application, where water was

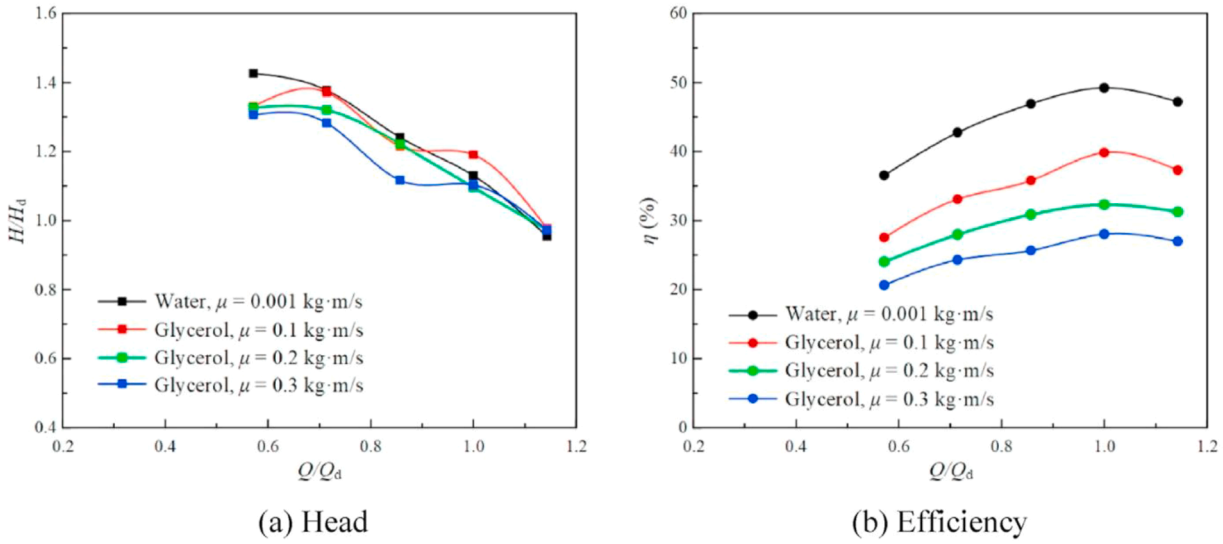

Fig. 12. Comparison of head and efficiency with increasing fluid viscosity reprinted with permission from Ref. [48].

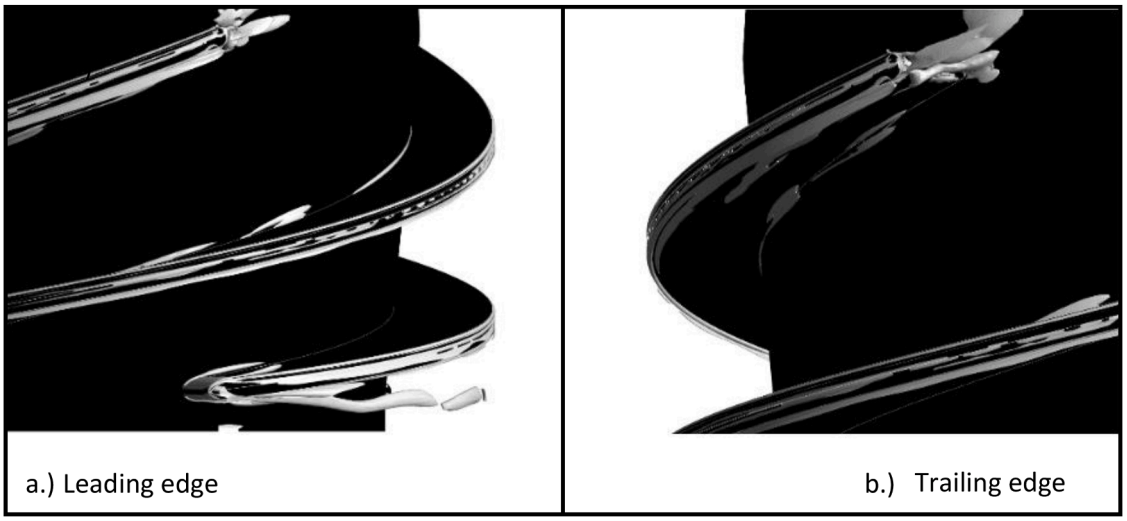

Fig. 13. Vortex shape at the leading and trailing edge of the multiphase impeller [50].

utilised as the motive fluid. Configuration 6 in Table 1 illustrates the set of parameters that reach a significantly higher BEP of 39.95 % with a relatively high head ratio of 0.37. It was reported that the variation in the pump pressure had a minimal effect on the sand suction capacity, whereas the rise in pump pressure had a corresponding increase in the lifting capacity. It is expected that the sand flushing will exhibit higher efficiency compared to the viscous emulsified oil handling in a jet pump system, owing to a lower flow resistance and absence of shear-dependent characteristics of the emulsified oil. The variation in the geometric and operational parameters within the jet pump, as presented in Table 1, demonstrates a noteworthy influence on both efficiency and head ratio. However, more comprehensive statistical data would be beneficial to quantify the relative impact of each parameter on the overall performance of the jet pump. The jet pumps are generally not popular for high efficiency but are commonly used in borehole applications where reliability is prioritised.

Jia et al. [55] investigated the impact of jet pump structure on its operating limit. An experiment was carried out to examine the influence of structural parameters and the flow ratio of the pump when working within its operating range. Water and two foaming agents (A and B for dust suppression and firefighting) were used as the secondary fluid. The authors also conducted a CFD analysis to study the distribution of pressure, velocity, rate of turbulent dissipation and vapour bubbles. The results showed that the pump was limited by cavitation due to overlapping turbulence and the low-pressure region at the discharge nozzle. When vapour bubbles due to cavitation were predominant at the cross-section close to the diffuser, it was noticed that the pump had reached its limit. In the experiment, nine jet pumps with different nozzle diameters were tested and studied. It was noticed that an increase in the secondary flow led to a rapid drop in the critical pressure ratio. Hence, empirical curves could be integrated to optimise the area ratio of the resulting flow ratio. From Fujita et al. [52] investigation, it can be deduced that the area-to-flow ratio of jet pumps has a beneficial and significant influence on the pump critical pressure ratio, pump limit and pump reliability. Liang et al. [56] further evaluates the application of gas motive power on the effect of the new annular jet pump (NAJP) and the conventional annular jet pump (CAJP), quantifying the performance by the cyclonic effect, droplet break ratio and efficiency of the jet pump. The NAJP differs from the CAJP by the implementation of the static mixer, which influenced the internal flow pattern as depicted in Fig. 16. The cyclonic effect of the static mixer at the suction chamber of the NAJP influenced the fluid mixture in the following three stages:

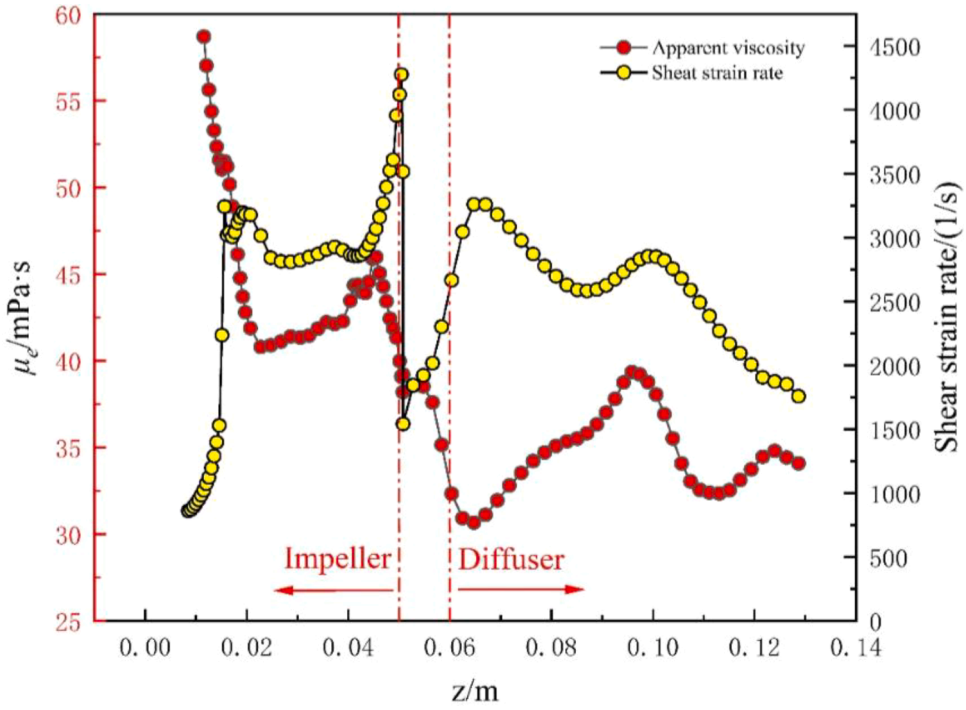

Fig. 14. Characteristics of apparent viscosity and shear strain rate across the flow channel of the multiphase pump [51].

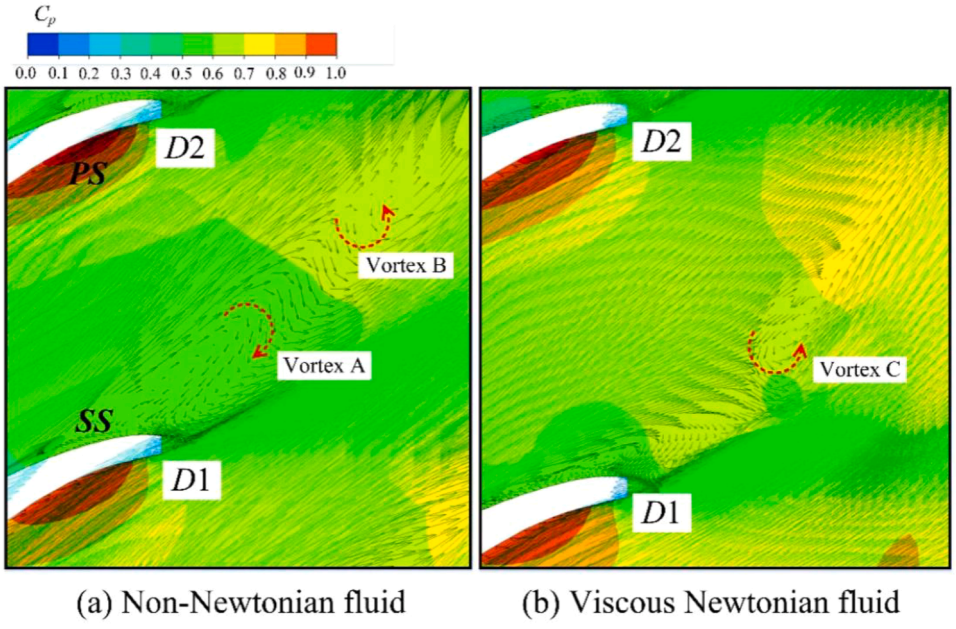

Fig. 15. Pressure and velocity distribution across the impeller of the multiphase pump [51].

Table 1
Parametric analysis of the jet pump performance across varying mixing tube diameters with water as the motive fluid.

Configuration	Mixing tube diameter (d_m) mm	Area Ratio (R)	Spacing between nozzle and mixing tube (S) mm	Discharge ratio (M)	Head ratio (N)	BEP %	Fluid type	References
1	38	0.2	13.2	0.62	0.23	14.1	Viscous	[53]
2	32	0.282	23	0.68	0.289	21	Emulsified oil	
3	28.2	0.363	24.25	0.78	0.299	23.5		
4	25.9	0.431	29.8	0.69	0.37	24.5		
5	24	0.502	28.5	0.75	0.38	25.1		
6	30	0.280	30	1.07	0.37	39.95	Sand	[54]

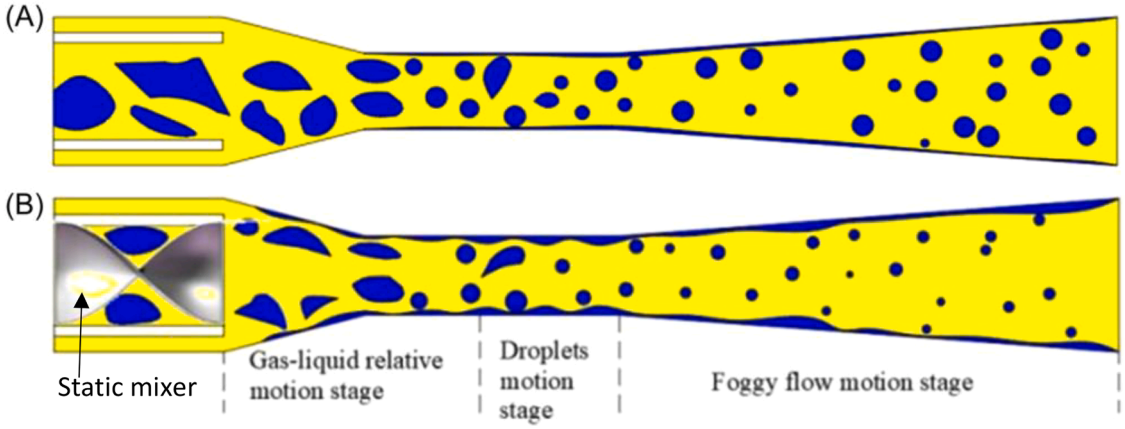

Fig. 16. Internal fluid dynamics of the annular jet pump. (A) conventional annular jet pump-CAJP, (B) new annular jet pump-NAJP [56].

- Gas-liquid relative motion stage - at low velocity, the entrained gas and liquid mixture breaks into smaller particles as they move from the suction chamber to the throat.
- Droplet motion stage - the gas acquires an increase in kinetic energy at the throat, inducing shear stress on the liquid, resulting in pulsation as the liquid disperses into smaller droplets.
- Foggy flow motion stage - the smaller droplets of the gas-liquid mixture move to the diffuser, decelerate and gains pressure toward the well-head. The breakdown of the mixture into droplets enhances the efficiency of the fluid transport in the jet pump.

The cyclonic effect generated by the static mixer augments the vortex motion within the Jet pump, which enhances fluid mixing and droplet breakup, thereby facilitating momentum transfer and improving the overall efficiency.

The effect of the static mixer at the NAJP significantly improved the suction at BEF of 37 % when compared to the CAJP BEP of 28.3 %; however, it had a steady reduction in the head as illustrated in Fig. 17. The observed performance trend is attributed to the cyclonic effect, which enhanced the mass flow rate, leading to an increase in the discharge head loss.

While the study carried out by Liang et al. [56] offers significant insight into the application of a static mixer in the jet pump, it will be beneficial to evaluate the performance characteristics of the number of vanes, vane angles and pitch angles over a vast parametric performance index to facilitate a robust insight into the design combinations suitable for a specific application. Special-effect jet pumps offer strong passability for viscous, multiphase, and solid-laden fluids, aided by high-temperature actuation and robust suction. They are useful in oil recovery, wastewater handling, dust suppression, well-dewatering and chemical processing applications. Their main disadvantages are sensitivity to design parameters, power consumption and susceptibility to cavitation. Optimising the geometry of the wetted part is a key strategy for improving efficiency, extending operating limits, and enhancing reliability.

Based on the review of various centrifugal, multiphase and jet pumps, Table 2 compares their efficiency when handling viscous fluids of different densities and rheological properties. The data shows a clear trend: as viscosity and density increased, particularly with pseudoplastic or high-viscosity fluids. Efficiency drops sharply (from 58 % at 110 cP to around 20–22 % at viscosities above 300 cP), reflecting structural limitations in the dynamic pump design. However, the jet pump exhibits a relatively higher efficiency of 39.95 % for sand extraction applications owing to improved momentum transfer due to minimal moving parts.

2.4. Tesla disc pump

Owing to the desirable characteristics of the Tesla disc pump, it is essential to investigate the causes of the characteristic low head and global efficiency. Since this pump type is not widely used in industrial applications, it is essential to understand the pump characteristics when handling solid, liquid and gaseous fluids. Engin et al. [57] conducted an

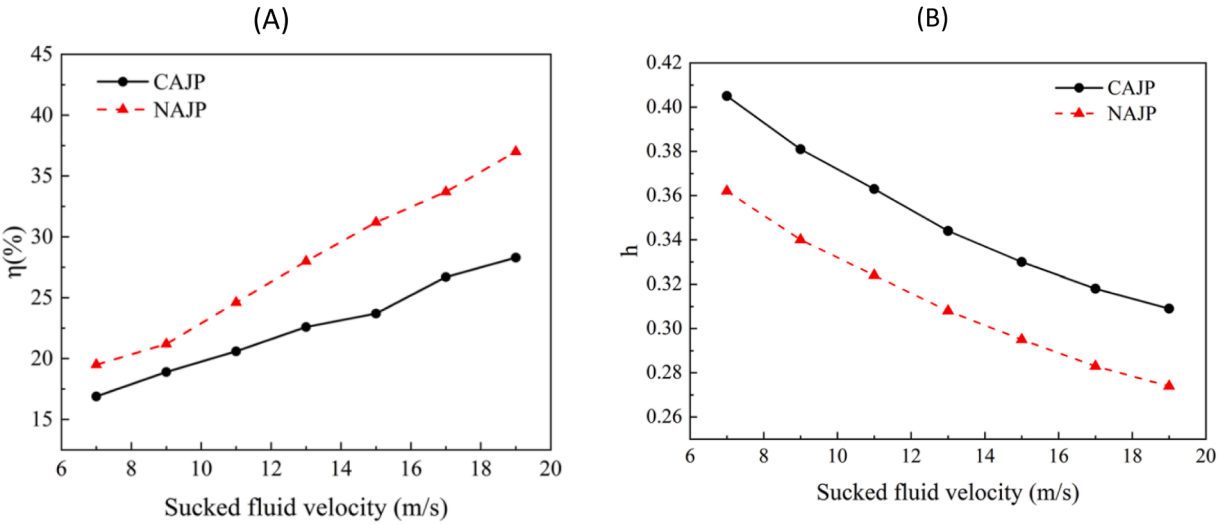

Fig. 17. Illustrates the comparison between CAJP and NAJP: A. suction velocity to efficiency, B. suction velocity to head [56].

Table 2
Rotodynamic pump comparison for various viscous and non-Newtonian applications.

References	Method	Pump type	Pumping Fluid type	Fluid Density (Kg/m^3)	Fluid viscosity (cP)	Efficiency (%)
Buratto et al. [43]	CFD	Centrifugal pump	Tomatoes	1100	110	58
Liu et al. [48]	CFD	Multiphase pump	Glycerol 1	1180	100	38
Lui et al. [48]	CFD	Multiphase pump	Glycerol 2	1330	300	20.5
Torabi et al. [47]	CFD	Centrifugal pump	Oil	700	24,500	22
Jia et al. [54]	Experiment	Jet pump	Sand	2650	1.5	39.95

experimental study of 2D modelling on the airflow between a co-rotating parallel disc fan by applying the conservation of angular momentum. In the experiment, the number of discs on the disc fan was varied with different inter-disc spacing. It was run with air at four different speeds, intended to study the characteristics of a disc propulsion system. The empirical relationship showed the factors that affect efficiency in a disc fan. It demonstrated that the relative loss in efficiency was associated with low viscosity due to the nature of the fluid (air), tangential flow due to disk spacing, and significant mechanical energy losses at both inlet and outlet due to low disc response to shaft speed.

It can be deduced that the loss of pressure head in a Tesla disc propulsion system was due to the predominant vortices formed in the inter-disc spacing, which resulted in the conservation of angular momentum, high static pressure at the inlet and low-pressure-head at the outlet. Since the disc pack operates by viscous drag and boundary layers, low viscosity fluid such as air cannot be lifted efficiently due to low magnitude caused by a poor energy transfer in the fluid. The energy transfer weakens even further as disc channels increase in width. Since the Tesla disc pump operates at high inlet pressure, high static pressure at the inlet will cause the net positive suction head required (NPSHr) to be greater than the net positive suction head available (NPSHa), ultimately reducing the pump performance and probably causing a cavitation condition. Furthermore, since the first generation of the Tesla disc pump is not incorporated with complex blades and guide vanes like other centrifugal pumps, it tends to be more susceptible to turbulence-induced vorticity.

John and Hanas [58] investigated the performance of the Tesla disc pump in different petroleum refinery plants. In the experiment, three Tesla pumps were installed in three different refinery plants. Two of the pumps encountered some failures resulting from high-pressure sensitivity and turbulence between the disc impellers. The conditions where the two pumps encountered failures in the refinery plants were the coke drum condensate (DCU) and heavy slope oil charge to the crude pump. Further experimental results by Heng et al. [38] showed that the Tesla disc pump was sensitive to cavitation at lower inlet pressure, where water was the working fluid. It was also stated that adding more discs to the impeller pack increased the flow rate alone; the head delivery and global efficiency remained low. However, Figueira et al. [59] experiment on designing a bladeless disc impeller for abrasive application (water and silicon carbide as working fluid) depicted that adding more discs to the impeller further augments the global efficiency of the pump. The experiment, as described in Fig. 18, also showed the presence of wear due to cavitation; it appears that the cavitation resulted from high static pressure at the inlet due to the nature of the abrasive fluid, whereas the parallel discs appear to remain intact.

Ideally, rotodynamic pumps convert flow to pressure and if the flow is augmented, it is expected to influence the head and efficiency of the disc pump. However, the efficiency of the Tesla bladed disc pumps are also subject to the working condition and rheology of the working fluid. With a low-viscosity fluid like water, the disc pump may be limited to a specific head and efficiency. Hence, the rise in flow rate may have no beneficial effect due to velocity slip induced by low energy transfer. However, for highly abrasive pulp composed of silicon carbide, the increase in disc number, which augments flow rate, should improve the global efficiency due to a more robust energy transfer and boundary layers. Fig. 19 describes the experimental result of the Tesla disc pump operating with 40/60 % propylene glycol-water mixture at 2500 rpm, where the increase in the disc channels from 5 thou (0.005 inches) to 15 thou (0.015 inches) had a progressive improvement in both head and efficiency, but began to decline on approaching higher disc spacing of 20 thou (0.02 inches). The trend was consistent across impeller speed, ranging from 2500 rpm to 3600 rpm [60]. It can be inferred that the disc spacing follows a characteristic performance trend where the optimal disc spacing depends on the fluid properties.

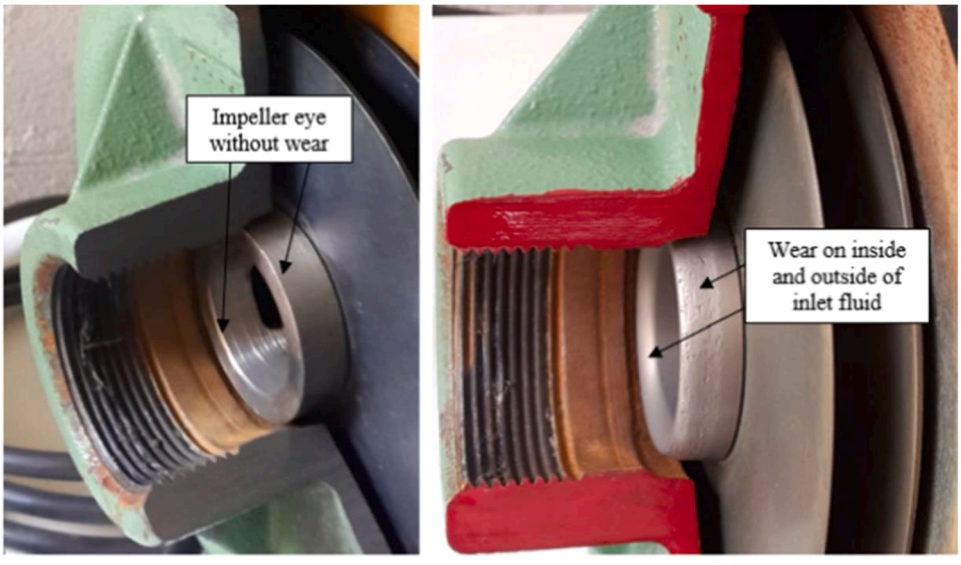

Fig. 18. Bladeless disc impeller: (a) before and (b) after a mixture of silicon carbide and water application, reprinted with permission from Ref. [59].

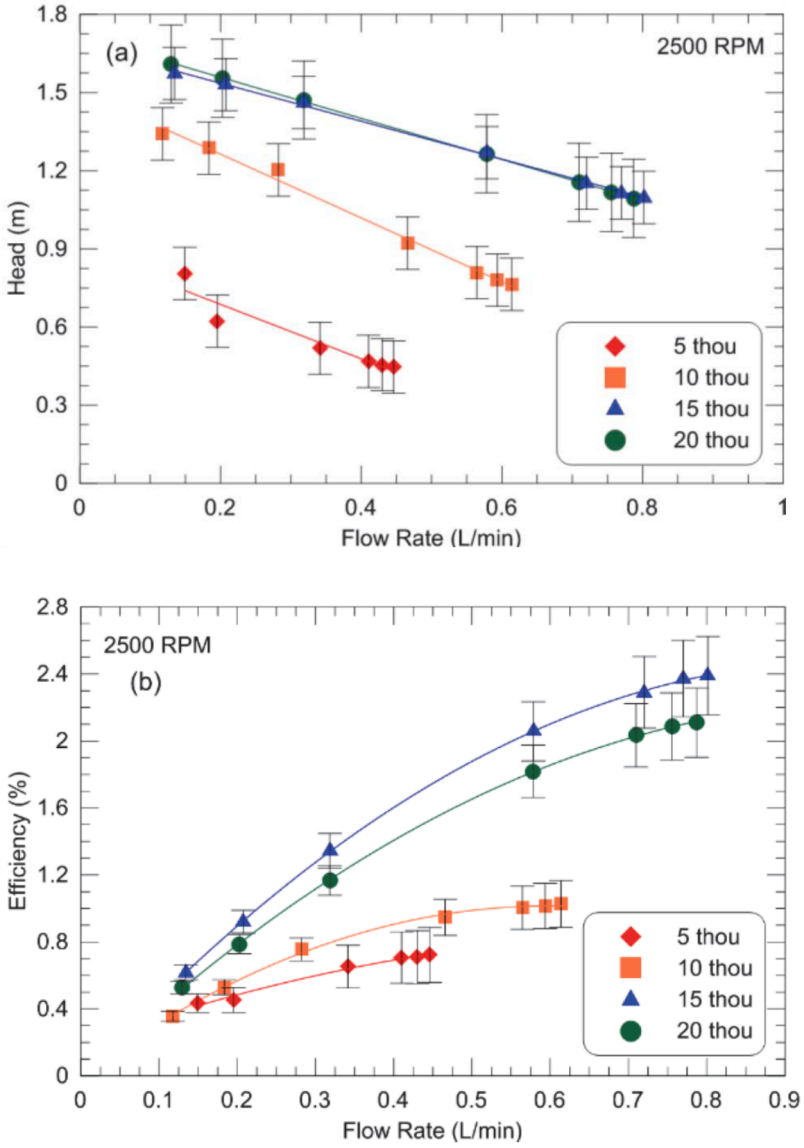

Fig. 19. Head and Efficiency curve of the Tesla disc pump at varying disc spacing [60].

Dodsworth et al. [60] validated a CFD investigation on the impact of viscosity on the Tesla disc pump, where the working fluid, water, was compared with a viscous mixture of propylene glycol and water. The results showed that denser boundary layers were generated during the viscous application between the discs, and a significantly higher efficiency was noticed at a lower speed. The study carried out by John and Hanas [58] further illustrated that the BEP for viscous application typically range from 40 % to 55 % and can reach a higher range of 60 % at its best performance. Furthermore, no significant vibration was noticed, indicating the non-likelihood. The Tesla disc pump had better efficiency than the centrifugal pump when handling a viscosity greater than 350 cp. It can efficiently handle viscosity up to 100,000 cP, but may encounter deficiencies when it exceeds 100,000 cP. It was further stated that the incorporation of guide vanes to the disc impeller augmented viscous drag and boundary layer thickness without distorting the characteristic laminar flow of the disc pump, resulting in a further increase in flow rate, head and global efficiency. Cheremushkin et al. [61] stated that adding radial vanes to the disc impeller augments the head and efficiency for several viscous applications. At low viscosity, head and efficiency were increased by 20 m and 30 %, respectively. The experiment by Martínez-Díaz et al. [37] explored the different shapes of radial blade cross-sections intended to augment the pump efficiency. A rectangular, circular and square-shaped blade was tested, and it was found that the square cross-sectioned blade promoted an optimised vortex circulation, which increased inter-disc energy transfer. Consequently, more head and efficiency were observed in the rectangular blades compared to other blade cross-sections.

Fig. 20 describes the effect of the new generation impeller as it compares with a conceptual design [62]. It was deduced that the first (bladeless) and the second (bladed) generation disc impeller had distinct advantages; the bladeless disc impeller was said to have better buffer layers, while the bladed impeller had better overall performance. The study of a conceptual impeller design with curved blades having a conical transition from the inlet, as in Fig. 20b, was said to have an improved head and efficiency by 4 m and 2 % compared to the current state of impeller design, as shown in Fig. 20a. During abrasive application for the bladed disc impeller, it was found that the solid particles settled on the smooth disc surface between each blade and did not settle on the bladed surface [63]. It is inferred that for disparate fluids of liquid and solid, the liquid phase generates boundary layers across the disc and bladed surface while the solid phase generates boundary layers between each blade on the disc surface, owing to the flowability and density of

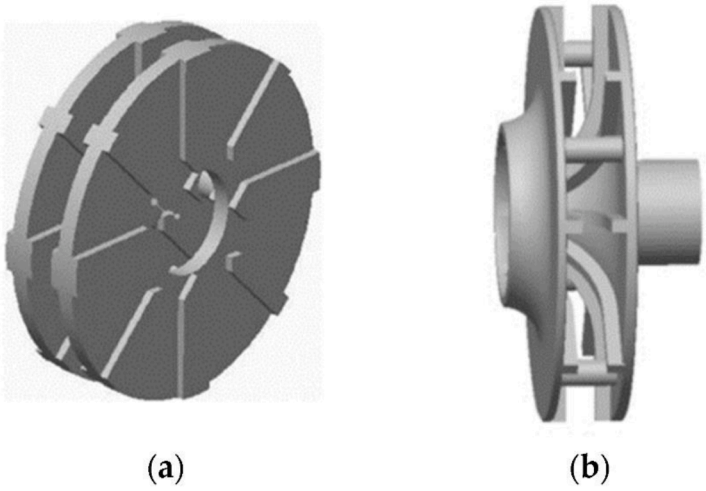

Fig. 20. a – Current disc impeller model; b – Conceptual disc impeller model [62].

the liquid media, the permeability and rigidity of the solid media.

Tesla disc pumps are proven to be highly effective for viscous, abrasive, and multiphase fluids, offering robust passability and simplicity in design and modular design improvements. However, their main limitations are low head and efficiency, which worsen with low-viscosity fluids. It has been articulated that by optimising the number of discs, discs spacing and incorporating guide vanes or radial blades, the performance can be significantly enhanced, making the Tesla disc pump a versatile solution for specialised pumping challenges.

Table 3 illustrates a gradual decline in boundary layer thickness as rotational speed increased. It demonstrates that a greater viscosity is experienced at lower disc speeds at the laminar and turbulent conditions, suggesting that the disc impeller will be more efficient at lower speeds as viscous drag and boundary layers are strengthened. Furthermore, the likelihood of impingement and corrosion is reduced by a larger inter-disc buffer layer, which improves fluid flow and minimises wear.

Table 3 also shows that increasing the disc spacing can lead to higher inter-disc turbulence, though the relationship between spacing and turbulence depends on the fluid flow conditions. Therefore, it is important to match the disc spacing to the fluid viscosity to optimise pump efficiency. It is known that the non-Newtonian property of a fluid determines its internal resistance to motion. Hence, it is difficult to pump viscous fluids as they often have low velocities and complex rheology compared to fluids with low viscosity, resulting in time-dependent viscosity and high internal friction among the fluid molecules relative to the surrounding surfaces [64]. Table 4 presents a broad range of industrial viscous fluids that can be effectively handled by the Tesla disc pump. This includes both Newtonian and non-Newtonian fluids, with densities that range from 997 kg/m^3 for water to 13,600 kg/m^3 for mercury. The viscosity spans from fluid with low viscosity to such as water (1 cP), to highly viscous materials, such as window putty, which ranges up to 100 million cP. Notably, the Tesla disc pump demonstrates good versatility in handling a wide range of fluid applications where rheology ranged from low-viscosity Newtonian fluids to complex, highly viscous non-Newtonian substances.

Table 3
Characteristics of turbulence and inter-disc boundary layer thickness relative to disc spacing and rotational speed for polypropylene glycol and water [60].

Rotational speed (RPM)	Inter-disc boundary layer thickness		Reynolds number of discs Spacing (mm)			
	Laminar-BL thickness (mm)	Turbulent-BL thickness (mm)	0.13 mm	0.25 mm	0.38 mm	0.51 mm
2500	0.52	65.53	129.2	258.5	387.7	516.9
3000	0.48	63.25	155.1	310.2	465.3	620.3
3600	0.43	60.96	186.1	372.2	558.3	744.4

2.5. Positive displacement pump

Fluids that exhibit high viscosity and non-Newtonian properties present unique challenges to both reciprocating and rotary PD pumps, as their flow behaviour significantly deviates from that of traditional Newtonian fluids. This section discusses the interaction between the complex fluids and the mechanisms of the various positive-displacement pumps for highly viscous and non-Newtonian fluids.

2.5.1. Reciprocating positive displacement pumps

As reciprocating PD pumps have a high tolerance for high viscosity applications, they encounter issues when these viscous fluids exhibit non-Newtonian properties.

The reciprocating PD pump consists of a double-action system where two cylinders move in opposite directions, intended to deliver a more stable flow output [31]. Typical plunger or piston-based PD pumps have a maximum viscosity range of 1500 Pa.s and hydraulic-powered diaphragm pumps have a maximum viscosity of 2000 pa.s [67]. Although the reciprocating PD pumps have a significantly higher tolerance and efficiency for highly viscous applications compared to other pumps, they often lose efficiency due to their structural and mechanical complexity. The experimental study of a plunger reciprocating pump with a characteristic ultra-high pressure [68] demonstrated that lag angles on valves had a noticeable impact on the overall efficiency of the pump. These lag angles were caused by; pressure drop due to the relationship between the actuator (plunger, piston, or diaphragm) and valves, reduced fluid volume in the working chamber, increased work volume due to elastic deformation of the working chamber and variable height clearance conditions [69]. A CFD study of the internal flow in piston PD pumps for multiphase application demonstrated a lag phenomenon observed at the opening and closing valves at the inlet and outlet [70]. Milani et al. [71] stated that the dynamic phenomenon and the operating temperature of the reciprocating pump must be accounted for to meet the required performance index. Investigations by Zhu et al. [6] showed that the efficient movement of the actuating mechanism was highly influenced by the disc valves, as the poor response of the disc valves may lead to cavitation, poor efficiency and complete failure of the pump. When the reciprocating PD pump handles high-viscosity fluids with non-Newtonian properties, temperature and shear stress directly influence the fluid viscosity, potentially inducing transient fluid behaviours and consequently limiting the performance of the dynamic

Table 4
Fluid properties and application for temperature in the range of 23 °C, data retrieved from current study, viscous scale reference guide and fluid viscosity chart [65,66].

Fluid	Rheology	Density (kg/m^3)	Viscosity (cPs)	Industrial application	Pump application
Water	Newtonian	997	1.0	Food production, industrial multi-purpose processing, energy generation, cleaning and cooling etc.	Tesla disc pump
Mercury	Newtonian	13.6×10^3	1.5	Batteries, semi-conductors, temperature and pressure gauge production, medical appliances etc.	Centrifugal pumps.
Polymer	Non-Newtonian	1104	1.94	Plastic bag, synthetic clothing, pipes, and tank production etc.	Tesla disc pump
Whole Milk	Newtonian	1035	2.127	Production of dairy, yogurts, cream, cakes, cheese, butter etc.	Tesla disc pump
Olive Oil	Newtonian	917.2	84		Tesla disc pump
Unfilled Rigid Urethane Resin	Non-Newtonian	1000 – 1300	80 – 120	Wide range of plastic production, casting etc.	Tesla disc pump
Motor Oil (SAE 50)	Non-Newtonian	1080	540	Lubricant for diesel powered engines	Tesla disc pump
Glycerine		1250	1490	Pharmaceutical application, resin, and plastic production etc.	
Motor Oil (SAE 60)	Non-Newtonian	1330	1000 – 2000	General domestic lubricants	Tesla disc pump
Water Base Paint	Non-Newtonian	1600	2400	Finishing of woods, metals, house interiors and exteriors etc.	Tesla disc pump
Pourable Urethane Rubbers	Non-Newtonian	20 – 29	1000 – 3000	Surface finishing, adhesive bonding agent, casting etc.	Tesla disc pump
Tomato Puree	Non-Newtonian	1100	50,000	Food production	Tesla disc pump
Petroleum Jelly	Non-Newtonian	900	64,000	Automotive and general industrial application, production of Vaseline, rubber etc.	Tesla disc pump
Peanut Butter	Non-Newtonian	1090.5	250,000	Food production	Tesla disc pump
Window Putty	Non-Newtonian	929	100,000,000	Wood frames, glass finishing, sealant, glazing etc.	Tesla disc pump

parts within the pump [72]. An incorrect check valve movement in a reciprocating PD pump delays fluid flow at the inlet and outlet. It will consequently slow down the working mechanism of the pump and could cause a cavitation condition when the NPSHr becomes greater than the NPSHa. Response from check valves in the reciprocating PD pump may result from the variable viscosity in the working fluid, as variation in flow resistance can affect the responses of the check valve. It is complicated to design a variable valve spring stiffness that will have a perfect response to all ranges of viscosity; however, the spring stiffness can be designed for a specific range of viscosity. Josifovic et al. [5] research on multi-cylinder pumps demonstrated that the valve responses in the pump had some dynamic fluctuations, which were linked to a phenomenal change in pressure. It was confirmed that variations in fluid properties, such as density, bulk modulus and operating conditions, can affect valve responses. The authors suggested that a valve control mechanism would improve valve stability. However, such optimisation is expected to increase its complexity and affect practicality in terms of cost of purchase and maintenance. Zhu et al. [6] compared a typical plunger and an optimised plunger pump type. The valves' structure was redesigned in the optimised plunger pump, and a variable spring stiffness was integrated. The results demonstrated that valve optimisation by variable spring stiffness significantly impacted the pump's overall efficiency. Delayed valve displacement was found to be influenced by valve weight and spring stiffness. Gökçe [33] added that at the BEP, an increased spring stiffness with a shorter valve displacement had a corresponding increase in volumetric and hydraulic efficiency by 7 % and 4 %, respectively. Though Zhu et al. [6] and Gökçe [33] explicitly carried out investigation on the optimisation of spring stiffness to improve pump performance, there is a great possibility that the optimised check valve may not be effective for all types of viscous and non-Newtonian fluids. Further investigation may be required to understand the range and viscosity limit for a specified valve spring stiffness and performance prediction at a variety of temperatures. The application of a 1D modelling tool can be utilised as a prediction tool for system-level optimisation of pumps for varying temperatures [73].

2.5.2. Rotary positive displacement pumps

Rotary pumps differ from reciprocating pumps as they utilise a rotational actuating mechanism. The rotating components, which operate by trapping and releasing fluids at a higher pressure, also face difficulties when handling viscous fluids with non-Newtonian properties. Although this pump type does not require mechanical check valves, they are prone to issues like seal wear, improper flow circulation and cavitation. Those issues are particularly pronounced for applications where viscous fluids exhibit non-Newtonian properties. Frosina et al. [74] investigated the adaptability of a slide vane PD pump as an oil pump in a high-performance internal combustion engine. It was found that the flow rate was limited due to flow recirculation, high rotating speed and relief valve interaction and other nebulous factors. However, better flow circulation and efficiency were reached at fewer rotations, cavitation was noticed at the pump's vanes, but the cavitation's cause was unclear. It is suspected that the eccentric operating system of the pump will generate some pressure difference, which could result in cavitation. Cheng et al. [75] suggested that the presence of a cavity at the discharge and suction was due to pressure distribution across the pump, which resulted from the rotation of the cylindrical vanes.

Table 5 is a comparison of the maximum viscosity that the specified pump can handle. However, these values are tentative, pending the size, design and working conditions. Table 5 demonstrated that PD pumps had the highest capacity for viscous application, and amongst rotodynamic pumps, the Tesla disc pump had higher capacity than the centrifugal pump.

In summary, centrifugal pumps are feasible and more efficient for fluid with low viscosity, but performance and reliability decline with the increase in fluid viscosity. Whereas PD pumps are more practical for

Table 5
Peak viscosity comparison.

Pump type	Peak viscosity (cp)	
Plunger/piston PD pump	2000,000	Worldpumps [67]
Diaphragm PD pump	1500,000	Worldpumps [67]
Tesla disc pump	100,000	Peter et al. [58]
Centrifugal pump (Enhanced impellers)	1000	Torabi et al. [47]

fluids with high viscosity however, the mechanical complexity, such as valves and spring designs, are not universally adaptable to all viscosity dynamics. In contrast, among rotodynamic pumps, the Tesla disc pump is suitable for fluids with high viscosity and requires little maintenance. However, the efficiency of the Tesla disc pump declines primarily due to hydraulic and mechanical losses from the open tolerance. It can be concluded that the selection of pumps largely depends on the application. However, this study has also demonstrated the impact of geometric optimisation on the pump performance.

3. Market analysis of rotodynamic and PD pumps

The life cycle cost (LCC) of industrial pumps is critical as they account for all elements of the pump from purchase down to scrapping, giving a holistic view that enables industries to understand the long-term cost implications before a pump is purchased. The LCC of a pump draws a conclusion from the sum of the initial cost, installation/commissioning cost, energy and operational costs, maintenance and repair costs, downtime cost, environmental cost and end of life disposal cost [76].

For this analysis, the centrifugal and side channel pumps are collectively considered as a representative of rotodynamic pumps. The grouping is justified by their general mode of operation, where a rotating impeller adds kinetic energy to a fluid, creating a pressure difference from the inlet to the outlet. Similarly, the hydra cell, peristaltic and membrane piston are collectively considered to represent a subtype of diaphragm and reciprocating PD pump. The grouping is based on the following operating principle:

- Hydra cell pump - uses hydraulic actuated diaphragms, which embody the concept of diaphragm PD pumps, advantageous in smooth flow with minimal vibration [77].
- Membrane piston PD pumps utilise diaphragm membranes which are actuated in a reciprocating motion, embodying the reciprocating PD pump. They are applicable for corrosive, abrasive and sensitive fluids [78].
- Peristaltic pumps utilise rolling compression mechanisms, which act upon a flexible tube or membrane in the discharge of fluid [79]. While they are not distinctively classified as a reciprocating or diaphragm pump, they can be viewed as a type of PD pump, as they share the same fundamental operational principles as other pumps in this category. Passable fluid includes biological, viscous and complex fluids.

Table 6 shows a comparison of the LCC for five different industrial pumps. It considers two rotodynamic pumps and three PD pumps as previously discussed, which exhibit varying tolerance to fluid viscosity. Hence, a baseline LCC comparison was done considering the same working conditions using fluid with low viscosity. The cost of purchase, annual maintenance cost and LCC for 10 years are shown in Table 6 and are graphically represented in Fig. 21.

Fig. 21 shows that the peristaltic pump incurred the lowest cost of purchase. However, its annual and LCC rises significantly above the rotodynamic pumps. The peristaltic pump is a type of rotary PD pump which utilises flexible tubes for pumping viscous fluid while retaining the fluid integrity [80]. However, a huge amount often goes into the recalibration and replacement of the flexible tubes [81].

The centrifugal, side channel and hydra cell pumps appear to closely match each other when comparing the purchase, annual maintenance and LCC. However, it is expected that the centrifugal and side channel pumps will require significantly more maintenance and LCC as fluid viscosity increases. This is due to vibration, clogging and impingement resulting from the close tolerances and working mechanism of the centrifugal pumps. Whereas the hydra cell pump, which is categorised as the diaphragm PD pump will cost relatively less as they are more efficient for clean and viscous fluid [82]. However, the major LCC is likely to originate from the maintenance of the flexible membranes, springs and valves as discussed in Section 2.5.2.

The membrane piston pumps, which are categorised under the diaphragm piston PD pump [83] incurred the highest purchase, annual maintenance and LCC. Section 2.5.2 described that most of the failure that may contribute to the LCC originates from the seals wearing off over time, and moving parts such as the flexible membrane, valves and springs.

Table 7 depicts the maintenance intervals, cost and the number of years elapsed before failure occurred when the Tela disc pump was subjected to intense working conditions, with hot, abrasive and viscous application. While typical centrifugal pumps failed to handle those intense fluids, Table 7 demonstrates that the Tesla disc pump handled emulsion from the sludge oil with only two maintenance requirements over a 3-year span. Hot steam with abrasive content, such as grit from DCU coke drum condensate, required maintenance twice in 1.5 years. For highly abrasive and viscous fluid from CPI and heavy slop oil, 5 and 6 maintenance were required in 1 and 0.3 years, respectively. While these problematic fluids can be handled by many PD pumps, it is expected that maintenance costs will be relatively higher due to the number of moving parts, complexity and flexible materials as discussed in Sections 2.5.1 and 2.5.2.

From the comparison between Tables 6 and 7, it is seen that while the Tesla disc pump handled unclean fluids with viscosities of around 40 to 200 times higher than those managed by other pumps evaluated in Fig. 6, it still maintained a comparable annual maintenance cost among other PD and centrifugal pumps. This highlights the robustness and cost-effectiveness that the Tesla pump exhibits in challenging, high-viscosity fluid applications.

4. Conclusion

This study presents a comprehensive analysis of pump technologies, categorised into rotodynamic and PD pumps, including their market evaluation. The classification considered operating principles, performance characteristics, LCCs, and practical applications.

Table 6
LCC of a typical centrifugal pump and various types of PD pumps [76].

		Rotodynamic pump		PD pumps		
Parameters	Units	Centrifugal 32–200	Side channel	Hydra cell G10	Peristaltic	Membrane Piston
Flowrate	m^3/h	1.4	1.4	1.4	1.4	1.4
Head	m	50	50	50	50	50
Density	Kg/m^3	1000	1000	1000	1000	1000
Kin. viscosity	mm^2/s	1	1	1	1	1
Energy price (per kWh)	GBP	0.067	0.067	0.067	0.067	0.067
Operating hours (per year)	h	4000	4000	4000	4000	4000
Years of operation	–	10	10	10	10	10
Cost of purchase	GBP	2946.5	2822	2739	1633.44	7636
Annual maintenance cost	GBP	4108.5	4174.9	3918.43	8554.81	11,377.64
Life cycle costs (10 years)	GBP	7055	6996.9	6657.43	10,188.25	19,013.64

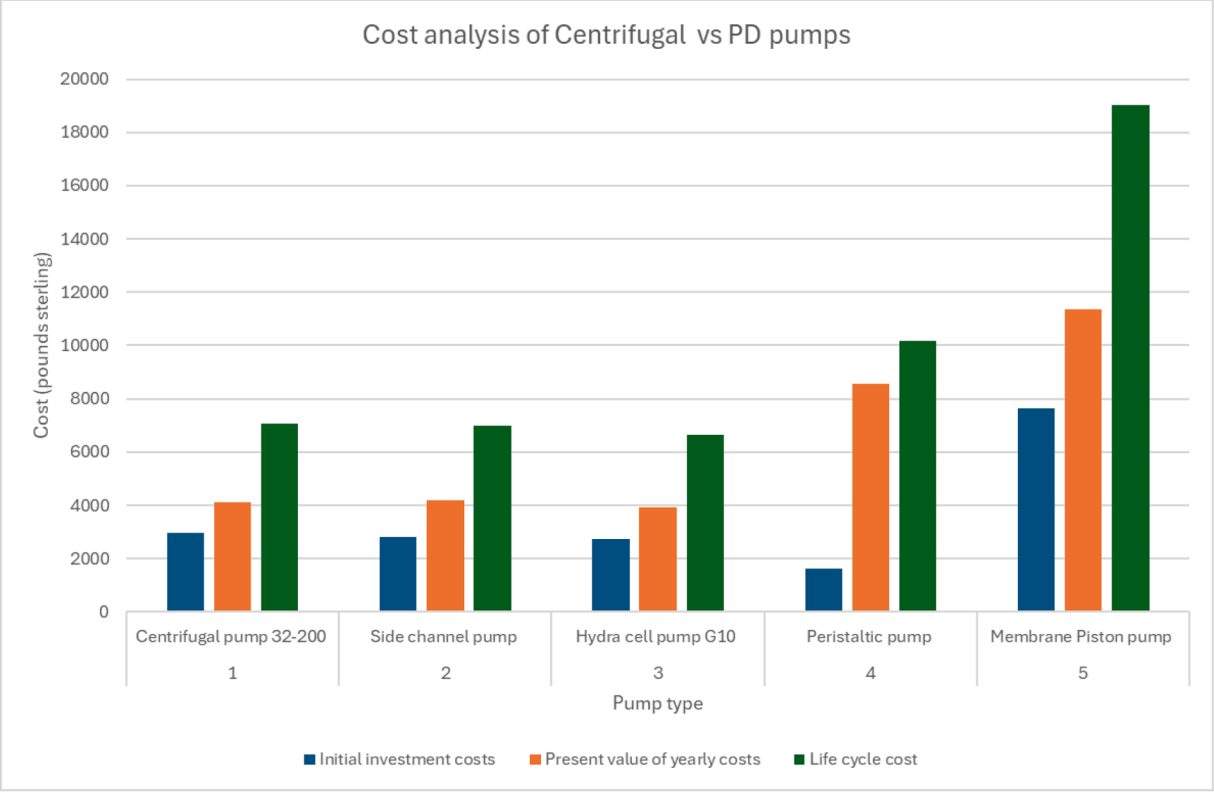

Fig. 21. Life Cycle cost analysis amongst different categories of PD and Rotodynamic pumps (Data taken from [76]).

Table 7
Maintenance cost of the Tesla disc pump [58,te29].

Pump Service	Fluid constituent	Number of maintenance performed	Mean time between failures (Years)	Kinematic viscosity (mm^2/s)	Total cost (GBP)
Sludge oil transfer	Emulsion, no solid	2	3	40	5353.92
DCU (coke drum condensate)	Hot + abrasive + steam	2	1.5	–	8699.34
CPI oil transfer	Highly abrasive	6	1	40	9107.28
Heavy slop oil charge to crude	Highly abrasive	5	0.3	200	14,000.22

A review of current technologies highlighted the pivotal role of structural design in determining pump performance for viscous and non-Newtonian slurry transport. Experimental and CFD analyses showed that optimising impeller and blade geometry in rotodynamic pumps significantly improved head, flow rate and efficiency. However, their performance deteriorated under high-viscosity or abrasive conditions due to increased resistance and energy losses.

1. Centrifugal pumps encounter performance challenges when handling fluids with higher viscosity and thixotropic characteristics, which exacerbate hydraulic losses, cavitation, clogging, and wear within the pump. Studies have shown up to 20 % efficiency reduction when compared to water application. Research has shown that the geometric optimisation of the volute tongue area, internal clearance and impeller vane design has a significant influence on the efficiency, radial forces, and flow stability within the pump. The practical viscosity limit for a typical centrifugal pump spans around 800 cP to 1000 cP, depending on the design; exceeding this value can lower efficiency and head due to increased disc friction, turbulence, and flow recirculation.
2. Multiphase pumps performed more efficiently with gas-liquid mixture and low viscosity applications. However, a performance decline was observed when operating with viscous and non-Newtonian fluids due to increased turbulence, vortex formation and hydraulic losses. The CFD investigations showed that the application of a highly viscous fluid reduced the flow rate and head due to an increasing turbulent kinetic energy and tip-leakage vortices at the edges of the impeller blades. This led to efficiency losses which range from around 50 % for water and 20 % for highly viscous glycerol. The non-Newtonian fluids exhibited shear-thinning behaviour, leading to a more complex vortex structure and greater pressure fluctuation, attributed to fluid thixotropy when compared to Newtonian fluids. The parametric optimisation of the blade geometry, tip clearance and materials are essential for extending the capabilities of the multiphase pump for high-viscosity or solid-laden flows and enhancing its integration with the jet pump system to handle slurry transport more effectively.
3. Special-effect jet pumps demonstrate strong capability in handling emulsified viscous, multiphase and solid-laden fluids, where performance was enhanced by high-temperature motive fluids, which lowered viscosity. In advanced designs with gas motive fluid, the implementation of static mixers enhanced cyclonic mixing and droplet breakup, which augmented efficiency. Experimental and parametric studies show that geometric variables such as the mixing tube diameter, area ratio and nozzle spacing had a strong influence on the discharge ratio, head ratio and BEP, which range from around

14.1 % to 25.1 % for viscous emulsions and 39.95 % for sand slurry application. While jet pumps generally have lower peak efficiencies than rotodynamic pumps, their lack of moving parts, high reliability, and tolerance for abrasive and heterogeneous mixtures make them valuable for oil recovery, slurry lifting, dust suppression and wastewater handling. Design optimisation remains essential to mitigate cavitation, extend operating limits and improve energy efficiency.

4. The Tesla disc pump exhibited better handling as fluid viscosity increased, attributed to an increase in boundary layer thickness and enhanced viscous drag within the impeller. A buffering effect originating from the boundary layers protected the impeller from abrasive impingement and augmented hydraulic efficiency. It was reported that the BEP of the Tesla disc pump can range up to 40 % to 55 %, while geometric optimisation of the wetted area can improve efficiency up to 60 %. Conceptual optimisation of the Tesla bladed impeller led to a 4 m increase in head and a 2 % efficiency gain over conventional designs. Further analysis of disc impeller configurations showed that bladeless designs encouraged thicker boundary layers, while radial blades improved momentum transfer, resulting in higher head and performance. Building on these findings, studies of solid-liquid flow revealed that solids tend to accumulate along the blade side, while the liquid phase remained uniformly distributed, indicating spatial variation as the boundary layer developed.
5. PD pumps, particularly reciprocating and rotary types, exhibit the highest tolerance for viscous and non-Newtonian fluids. The plunger and diaphragm pumps handled viscosities ranging from 1.5×10^6 cP to 2×10^6 cP. The reciprocating pumps maintained high efficiency in such applications but face performance losses due to valve response delays, spring stiffness limitations and mechanical complexity, prompting research into optimising valve designs and stiffness control. The rotary PD pump designs, such as vane pumps, do not include check valves but are prone to seal wear, recirculation and cavitation when handling complex fluids. Although PD pumps handled a wider range of fluid viscosity compared to the rotodynamic pumps, their adaptability was constrained by mechanical design limits, requiring application-specific optimisation of the key performance parameter, materials and control sensitivity, particularly for non-Newtonian fluid.
6. The LCC analysis, which compared the centrifugal and side channel (rotodynamic) pumps with various PD pumps, showed that while peristaltic pumps had the least purchase price, their high maintenance and tube replacement requirements increased the long-term costs. Centrifugal, side channel and hydra cell pumps exhibited a comparable LCC under low-viscosity conditions. As viscosity increases, it is expected that the rotodynamic pumps will incur higher costs due to higher maintenance demand. The membrane piston PD pumps had the highest purchase and operating costs, largely due to seals and moving-part wear. The Tesla disc pumps, although outside the baseline LCC table, demonstrated a superior robustness in abrasive, high kinematic viscosity applications ranging from 40 - 200 mm^2/s, while maintenance costs remained comparable to conventional PD and centrifugal pumps, highlighting the suitability of the Tesla disc pumps for challenging fluid applications common in slurry transport.

Geometric optimisation of wetted area in suitable pumps can generally improve overall performance. Moreover, the optimisation of the Tesla bladed disc pump may play a pivotal role in sustainable application for dense slurry transport, as they could potentially complement both rotodynamic and PD technologies in modern industrial systems. The sustainability of Tesla disc pump is attributed to extended service life, reduced frequency of part replacements and stable efficiency with slurry transport, reducing the long-term environmental and financial footprint compared to less durable pump types.

CRediT authorship contribution statement

Oscar Ifidon: Writing – review & editing, Writing – original draft, Methodology, Investigation, Formal analysis, Conceptualization. **Daya Shankar Pandey:** Writing – review & editing, Supervision, Methodology, Conceptualization. **Khurshid Ahmad:** Writing – review & editing. **Artur J. Jaworski:** Writing – review & editing, Supervision, Methodology, Conceptualization. **Faisal Asfand:** Writing – review & editing, Supervision, Methodology, Conceptualization.

Declaration of competing interest

The authors declare that they have no known competing financial interests or personal relationships that could have appeared to influence the work reported in this paper.

Data availability

Data will be made available on request.

References

[1] R. Francis, L. Phillips, Cost effective materials selection for pumps, Pump Eng. (2003) 44–49.
[2] D. Kernan, Pumps 101: operation, maintenance and monitoring basics, Monit. Control Group ITT (2009) 2–9.
[3] D.B. Parker, Positive displacement pumps-performance and application, in: Proceedings of the 11th International Pump Users Symposium, Turbomachinery Laboratories, Department of Mechanical Engineering, Texas A&M University, 1994.
[4] J. Pei, C. He, M. Lv, X. Huang, K. Shen, K. Bi, The valve motion characteristics of a reciprocating pump, Mech. Syst. Signal Process. 66–67 (2016) 657–664, https://doi.org/10.1016/j.ymssp.2015.06.013.
[5] A. Josifovic, J. Corney, B. Davies, Valve dynamics in multi-cylinder positive displacement pump model, in: *IEEE/ASME International Conference on Advanced Intelligent Mechatronics*, AIM, Institute of Electrical and Electronics Engineers Inc, 2015, pp. 35–41, https://doi.org/10.1109/AIM.2015.7222505. Aug.
[6] G. Zhu, S.M. Dong, Analysis on the performance improvement of reciprocating pump with variable stiffness valve using CFD, J. Appl. Fluid Mech. 13 (2) (2019) 387–400, https://doi.org/10.29252/jafm.13.02.30478.
[7] Michael smith Engineers, Useful information on positive displacement pumps. https://www.michael-smith-engineers.co.uk/resources/useful-info/positive-displacement-pumps, 2021.
[8] O.M. Elmardi and S. Khayal, "Pump types the effect of excessive oil-gasoline mixture on the acceleration of Bajaj Rickshaw vehicles view project mechanics of solids view project," 2017.
[9] K.C. Thin, K.M. Aye, Design and performance analysis of centrifugal pump, World Acad. Sci. Eng. Technol. (46) (2008) 422.
[10] Difficulties when pumping high viscosity fluids - EDDY pump. https://eddypump.com/education/difficulties-when-pumping-high-viscosity-fluids/, 2021.
[11] M. Issametova, A. Issametov, N. Tokmurzina-Kobernyak, Determination of centrifugal pump efficiency based on cradle cad evaluation experiment, J. Energy Mech. Eng. Trans. 1 (3) (2024) 41–46.
[12] H.M. Badr, W.H. Ahmed. *Pumping Machinery Theory and Practice*, John Wiley & Sons, 2015, https://doi.org/10.1002/9781118932094.
[13] D.P. Nolan, Pump types and applications. Firewater Pumps at Industrial Facilities, Elsevier, 2011, pp. 37–53, https://doi.org/10.1016/b978-1-4377-4471-2.00006-2.
[14] S. Kim, K.Y. Lee, J.H. Kim, J.H. Kim, U.H. Jung, Y.S. Choi, High performance hydraulic design techniques of mixed-flow pump impeller and diffuser, J. Mech. Sci. Technol. 29 (1) (2015) 227–240, https://doi.org/10.1007/s12206-014-1229-5. Jan.
[15] Y. Hao, L. Tan, Symmetrical and unsymmetrical tip clearances on cavitation performance and radial force of a mixed flow pump as turbine at pump mode, Renew. Energy 127 (2018) 368–376, https://doi.org/10.1016/j.renene.2018.04.072. Nov.
[16] V. Chhaya, V.G. Chhanya, P.J. Thoriya, Review on design improvement of mixed flow pump, Int. J. Adv. Eng. Res. Dev. 1 (2014) [Online]. Available, https://www.researchgate.net/publication/280571392.
[17] S. Srivastava, A.K. Roy, K. Kumar, Design of a mixed flow pump impeller and its validation using FEM analysis, Procedia Technol. 14 (2014) 181–187, https://doi.org/10.1016/j.protcy.2014.08.024.
[18] W. Zhang, Z. Yu, B. Zhu, Influence of tip clearance on pressure fluctuation in low specific speed mixed-flow pump passage, Energies 10 (2) (2017), https://doi.org/10.3390/en10020148.
[19] J. Nejadrajabali, A. Riasi, S.A. Nourbakhsh, Flow pattern analysis and performance improvement of regenerative flow pump using blade geometry modification, Int. J. Rotating Mach. 2016 (2016), https://doi.org/10.1155/2016/8628467.

[20] W. Cao, W. Li, Study on the performance improvement of axial flow pump's Saddle Zone by Using a Double Inlet Nozzle, Water 12 (5) (2020) 1493, https://doi.org/10.3390/w12051493.

[21] F.J. Quail, M. Stickland, A. Baumgartner. Design study of a novel regenerative pump using experimental and numerical techniques, Woodhead Publishing, 2010, pp. 2–7.

[22] T. Meakhail, S.O. Park, An improved theory for regenerative pump performance, Proc. Inst. Mech. Eng. A: J. Power Energy 219 (3) (2005) 213–222, https://doi.org/10.1243/095765005X7565. May.

[23] D.T. Hatzlavramldls, Modeling and design of jet pumps, in: SPE Annual Technical Conference and exhibition, 1991, pp. 413–416. Nov.

[24] E. Lisowski and H. Momeni, "Modelling of a jet pump with circumferential nozzles for large flow rates," vol. 10, no. 3, pp. 69–72, 2010.

[25] A. Gutierrez, "Calhoun: the NPS Institutional Archive electromagnetic pumps for liquid metals," 1965.

[26] J. Rosettani, W. Ahmed, P. Geddis, L. Wu, B. Clements, Experimental and numerical investigation of gas-liquid metal two-phase flow pumping, Int. J. Thermofluids 10 (2021), https://doi.org/10.1016/j.ijft.2021.100092. May.

[27] S. Kikuchi and K. Murakami, "Behavior of a new Dc electromagnetic pump using superconducting magnet," Sep. 1977.

[28] A.T. Al-Halhouli, M.I. Kilani, S. Büttgenbach, Development of a novel electromagnetic pump for biomedical applications, Sens. Actuators A: Phys. (2010) 172–176, https://doi.org/10.1016/j.sna.2010.02.001. Aug.

[29] Cranfield University, "A novel surface jet pump apparatus for the oil-and-gas and process industries." Accessed: Sep. 11, 2023. [Online]. Available: https://www.cranfield.ac.uk/business/develop-your-technology-and-products/license-our-technology/a-novel-surface-jet-pump-apparatus.

[30] H.H. Tackett, J.A. Cripe, G. Dyson, Positive displacement reciprocating pump fundamentals-power and direct acting types. https://hdl.handle.net/1969.1/163923.

[31] J.A. De Jongh and R.P.P. Rijs, *Pump design*. Academia, 2004.

[32] Michael Smith Engineers LTD, Useful information on positive displacement pumps, [Online], Accessed: 15 October 2025, Available: https://www.michael-smith-engineers.co.uk/resources/useful-info/positive-displacement-pumps.

[33] G. Gökçe, Performance evaluation and CFD analysis of a positive displacement diaphragm pump, MIDDLE EAST TECHNICAL UNIVERSITY, 2011.

[34] J.A. Kent, Numerical and Experimental Analysis of a TurboPiston Pump, University of New Orleans, 2010 [Online]. Available, https://scholarworks.uno.edu/td.

[35] H.D.S. Couto, J.B.F. Duarte, D. Bastos-Netto, The tesla turbine revisited, in: Proceedings of the Eighth Asia-Pacific International Symposium on Combustion and Energy Utilization, 2006, pp. 10–12. Sep.

[36] D. Blanchard, P. Ligrani, B. Gale, Single-disk and double-disk viscous micropumps, Sens. Actuators A: Phys. 122 (1) (2005) 149–158, https://doi.org/10.1016/j.sna.2005.03.072. *Elsevier*SepAccessed: Feb. 01, 2023. [Online]. Available.

[37] L. Martínez-Díaz, H.H. Herrera, L.M.C. González, N.V. Izquierdo, T.R. Carvajal, Effects of turbulization on the disc pump performance, Alex. Eng. J. 58 (3) (2019) 909–916, https://doi.org/10.1016/j.aej.2019.03.011. Sep.

[38] Y. Heng, et al., Tesla bladed pump (Disc Bladed Pump) preliminary experimental performance analysis, Energies 13 (18) (2020), https://doi.org/10.3390/en13184873. Sep.

[39] L. Alfa, Problem solving-centrifugal pumps inside view, Alfa Laval Kolding A/S (2010) 12–13. Aug.

[40] Uchida Norio, Imaichi Kensaku, Shirai Toshiaki, Radial force in the impeller of a centrifugal pump, Radial Force Impeller Centrif. Pump 14 (1971) 76.

[41] W. Zhou, Z. Zhao, T.S. Lee, S.H. Winoto, Investigation of flow through centrifugal pump impellers using computational fluid dynamics, Int. J. Rotating Mach. 9 (1) (2003) 49–61, https://doi.org/10.1080/10236210390147380.

[42] F. Orlandi, L. Montorsi, M. Milani, Cavitation Analysis Through CFD in Industrial pumps: A review, Elsevier B.V., 2023, https://doi.org/10.1016/j.ijft.2023.100506. Nov. 01.

[43] C. Buratto -M Pinelli -PR Spina -A Vaccari -C Verga, "CFD Study on Special Duty Centrifugal Pumps Operating With Viscous And Non-Newtonian Fluids," Madrid, Spain, 2015.

[44] M. Onica, S.N. Oliveira, M.A. Alves, and F.T. Pinho, "Microfluidic flows of viscoelastic fluids," 2012.

[45] M. Zaman, S. Ali, W. Abdul, Selection of a low-cost high efficiency centrifugal pump, in: Fifth International Conference on Aerospace Science & Engineering, IEEE, 2007, pp. 1–7.

[46] A. Berrada, K. Loudiyi, System Performance and testing. Gravity Energy Storage, Elsevier, 2019, pp. 105–139, https://doi.org/10.1016/b978-0-12-816717-5.00005-0.

[47] R. Torabi, S.A. Nourbakhsh, The effect of viscosity on performance of a low specific speed centrifugal pump, Int. J. Rotating Mach. 2016 (2016), https://doi.org/10.1155/2016/3878357.

[48] M. Liu, L. Tan, S. Cao, Influence of viscosity on energy performance and flow field of a multiphase pump, Renew. Energy 162 (2020) 1151–1160, https://doi.org/10.1016/j.renene.2020.08.129. Dec.

[49] K. Räbiger, T.M. Maksoud, J. Ward, G. Hausmann, Theoretical and experimental analysis of a multiphase screw pump, handling gas–liquid mixtures with very high gas volume fractions, Exp. Therm. Fluid Sci. (2008) 1694–1701, https://doi.org/10.1016/j.expthermflusci.2008.06.009.

[50] J. Zhang, L. Tan, Energy performance and pressure fluctuation of a multiphase pump with different gas volume fractions, Energies 11 (5) (2018), https://doi.org/10.3390/en11051216.

[51] L. Chen, Y. Yang, C. Peng, X. Zhang, Y. Gong, The influence of shear-thinning characteristics on multiphase pump vortex structure evolution, pressure fluctuation, and gas-solid distribution, Processes 12 (2) (2024), https://doi.org/10.3390/pr12020284. Feb.

[52] I. Fujita, Y. Muneo, Y. Saito, STEAM JET PUMP FOR OIL RECOVERY AND REFORMATION, Port and Airport Research Institute, 2021, pp. 589–593. Nov [Online]. Available, http://meridian.allenpress.com/iosc/article-pdf/2005/1/589/2348494/2169-3358-2005-1-589.pdf.

[53] S.K. Gugulothu, S. Manchikatla, Experimental and performance analysis of single nozzle jet pump with various mixing tubes, Int. J. Recent adv. Mech. Eng. 3 (4) (2014) 119–133, https://doi.org/10.14810/ijmech.2014.3411. Nov.

[54] X. Jia, H. Liao, Q. Hu, Y. He, Y. Wang, W. Niu, Optimization method of jet pump process parameters and experimental study on optimal parameter combinations, Processes 11 (10) (2023), https://doi.org/10.3390/pr11102841. Oct.

[55] X. Zhu, D. Wang, C. Xu, Y. Zhu, W. Zhou, F. He, Structure influence on jet pump operating limits, Chem. Eng. Sci. 192 (2018) 143–160, https://doi.org/10.1016/j.ces.2018.05.054. Dec.

[56] H. Liang, C. Li, J. Ma, L. Mu, X. Jiang, Study on improving liquid carrying performance of annular jet pump gas well with static mixer, Energy Sci. Eng. 12 (1) (2024) 70–86, https://doi.org/10.1002/ese3.1617. Jan.

[57] T. Engin, M. Özdemir, Ş. Çeşmeci, Design, testing and two-dimensional flow modeling of a multiple-disk fan, Exp. Therm. Fluid. Sci. 33 (8) (2009) 1180–1187, https://doi.org/10.1016/j.expthermflusci.2009.07.007.

[58] P. John, P. Hanas, Pumping machinery. DISC Pump -Type Pump Technology for Hard to Pump Applications, Texas A&M University, 2000, pp. 69–80.

[59] E.A. Figueira Júnior, C.H. de Freitas Oliveira, V.L. Borges, S.R. de Carvalho, Design of bladeless impellers for abrasive fluid pumping, J. Braz. Soc. Mech. Sci. Eng. 43 (4) (2021), https://doi.org/10.1007/s40430-021-02954-1. Apr.

[60] Dodsworth L. Operational parametric study of a prototype tesla pump [Master's thesis]. Halifax (NS): Dalhousie University; 2016. Available from: https://dalspace.library.dal.ca/items/e492b042-ea5e-4362-9131-306829294587.

[61] V. Cheremushkin, V. Lomakin, Development and research of hydraulic disk pump, in: IOP Conference Series: Materials Science and Engineering, Institute of Physics Publishing, 2019, https://doi.org/10.1088/1757-899X/492/1/012039. Mar.

[62] Y. Pei, Q. Liu, K.T. Ooi, Research on Energy-Efficient Disc Pumps: A Review on Physical Models and Energy Efficiency, Multidisciplinary Digital Publishing Institute (MDPI), 2023, https://doi.org/10.3390/machines11100954. Oct. 01.

[63] Y. Pei, Q. Liu, C. Wang, G. Wang, Analytical methods and verification of impeller outlet velocity slip of solid–Liquid disc pump with multi-type blades, Arab. J. Sci. Eng. 46 (7) (2021) 6835–6847, https://doi.org/10.1007/s13369-020-04951-3. Jul.

[64] F. Irgens, Rheology and Non-Newtonian Fluids, 1, Springer International Publishing., New York, 2014.

[65] Condor, "fluid viscosity centipoise (cP) chart, Accessed: Jan. 31, 2023. [Online]. Available, https://3819277.app.netsuite.com/core/media/media.nl?id=372800&c=3819277&h=6d930075efbea3a509c2&_xt=.pdf, 2019.

[66] Smooth-on, Viscosity scale reference guide, Accessed: Jan. 31, 2023. [Online]. Available, www.smooth-on.com, 2019.

[67] B. Edwin, L. Wolfgang, The Right Pump Lowers Total Cost of Ownership, Elsevier Ltd, 2007. Aug.02621762/07.

[68] T. Wang, G. Wang, L. Dai, L. Chen, S. Qiu, R. Li, Motion mechanism study on the valve disc of an ultra-high pressure reciprocating pump, Mech. Syst. Signal. Process. 160 (2021), https://doi.org/10.1016/j.ymssp.2021.107942. Nov.

[69] G. Muzzioli, F. Orlandi, M. Venturelli, M. Milani, L. Montorsi, CFD simulation of the slipper dynamics during variable displacement operations in a swash-plate type axial piston pump, Int. J. Thermofluids 24 (2024), https://doi.org/10.1016/j.ijft.2024.100992. Nov.

[70] Y. Ma, Y. Ni, H. Zhang, S. Zhou, H. Deng, Influence of valve's lag characteristic on pressure pulsation and performance of reciprocating multiphase pump, J. Pet. Sci. Eng. 164 (2018) 584–594, https://doi.org/10.1016/j.petrol.2018.02.007. May.

[71] M. Milani, L. Montorsi, M. Venturelli, A combined numerical approach for the thermal analysis of a piston water pump, Int. J. Thermofluids 7–8 (2020), https://doi.org/10.1016/j.ijft.2020.100050. Nov.

[72] D. Bossinov, G. Ramazanova, D. Turalina, Comparison of measured and calculated high-viscosity crude oil temperature values in a pipeline during continuous pumping and shutdown modes, Int. J. Thermofluids 24 (2024), https://doi.org/10.1016/j.ijft.2024.100950. Nov.

[73] D.T. Bantelay, G. Gebresenbet, B.T. Admasu, S.G. Gebeyehu, One-dimensional pump geometry prediction modeling for energy loss analysis of pumps working as turbines, Int. J. Thermofluids 21 (2024), https://doi.org/10.1016/j.ijft.2024.100562. Feb.

[74] E. Frosina, A. Senatore, D. Buono, M. Olivetti, A TRIDIMENSIONAL CFD analysis of the oil pump of an high performance engine, in: SAE Technical Papers, SAE International, 2014, https://doi.org/10.4271/2014-01-1712.

[75] Y. Cheng, X. Wang, W. Ur Rehman, T. Sun, H. Shahzad, H. Chai, Numerical simulation and experimental performance research of cylindrical vane pump, Proc. Inst. Mech. Eng. C. J. Mech. Eng. Sci. (2021), https://doi.org/10.1177/09544062211020037.

[76] F.-W. Hennecke, A Comparative Study of Pump Life Cycle Costs, Europump and the Hydraulic Institute, USA, 2001, pp. 20–27.

[77] Y. Anis, J. Houkal, M. Holl, R. Johnson, D. Meldrum, Diaphragm pico-liter pump for single-cell manipulation, Biomed. MicroDevices 13 (4) (2011) 651–659, https://doi.org/10.1007/s10544-011-9535-5. Aug.

[78] M.M. Gong, B.D. MacDonald, T. Vu Nguyen, D. Sinton, Hand-powered microfluidics: a membrane pump with a patient-to-chip syringe interface, Biomicrofluidics. 6 (4) (2012), https://doi.org/10.1063/1.4762851. Nov.

[79] X. Zhang, Z. Chen, Y. Huang, A valve-less microfluidic peristaltic pumping method, Biomicrofluidics. 9 (1) (2015), https://doi.org/10.1063/1.4907982. Feb.

[80] J. Klespitz and L. Kovács, "Peristaltic pumps - A review on working and control possibilities," 2014, pp. 191–194. doi: 10.1109/SAMI.2014.6822404.
[81] Michael Smith Engineers ltd, Michael Smith engineers ltd, Accessed: Feb. 01, 2023. [Online]. Available, www.michael-smith-engineers.co.uk, 1971.
[82] Wanner Engineering, "Hydra-cell pumps for high pressure cleaning dependable pump technology," www.hydra-cell.eu. Accessed: Feb. 08, 2023. [Online]. Available: www.hydra-cell.eu.
[83] D. Bach, F. Schmich, T. Masselter, T. Speck, A Review of Selected Pumping Systems in Nature and Engineering - Potential biomimetic Concepts for Improving Displacement Pumps and Pulsation Damping, Institute of Physics Publishing, 2015, https://doi.org/10.1088/1748-3190/10/5/051001. Sep. 03.